



HAL
open science

The Shewhart-type RZ control chart for monitoring the ratio of autocorrelated variables

Huu Du Nguyen, Adel Ahmadi Nadi, Kim Duc Tran, Philippe Castagliola, Giovanni Celano, Kim Phuc Tran

► To cite this version:

Huu Du Nguyen, Adel Ahmadi Nadi, Kim Duc Tran, Philippe Castagliola, Giovanni Celano, et al.. The Shewhart-type RZ control chart for monitoring the ratio of autocorrelated variables. *International Journal of Production Research*, 2023, 61 (20), pp.6746-6771. <10.1080/00207543.2022.2137594>. <hal-04184195>

HAL Id: hal-04184195

<https://hal.science/hal-04184195v1>

Submitted on 21 Aug 2023

HAL is a multi-disciplinary open access archive for the deposit and dissemination of scientific research documents, whether they are published or not. The documents may come from teaching and research institutions in France or abroad, or from public or private research centers.

L'archive ouverte pluridisciplinaire HAL, est destinée au dépôt et à la diffusion de documents scientifiques de niveau recherche, publiés ou non, émanant des établissements d'enseignement et de recherche français ou étrangers, des laboratoires publics ou privés.



HAL Authorization

ARTICLE TEMPLATE

The Shewhart-type RZ control chart for monitoring the ratio of autocorrelated variables

Huu Du Nguyen^a, Adel Ahmadi Nadi^b, Kim Duc Tran^c, Philippe Castagliola^d, Giovanni Celano^e, and Kim Phuc Tran^b

^aSchool of Applied Mathematics and Informatics, Hanoi University of Science and Technology, Hanoi, Vietnam; ^bUniv. Lille, ENSAIT, ULR 2461 - GEMTEX - Génie et Matériaux Textiles, F-59000 Lille, France; ^cInternational Research Institute for Artificial Intelligence and Data Science, Dong A University, Danang, Vietnam; ^dNantes Université & LS2N UMR CNRS 6004, Nantes, France; ^eUniversity of Catania, Department of Civil Engineering and Architecture, Catania, Italy

ARTICLE HISTORY

Compiled August 21, 2023

ABSTRACT

In many industrial manufacturing processes, the quality of products can depend on the relative amount between two quality characteristics X and Y . Often, this calls for the on-line monitoring of the ratio $Z = X/Y$ as a quality characteristic itself by means of a control chart. A large number of control charts monitoring the ratio have been investigated in the literature under the assumption of independent normal observations of the two quality characteristics. In practice, due to the high frequency in sensor data collection, both autocorrelation and cross-correlation between consecutive observations can exist for X and Y and should be modeled to protect against the false alarm rate inflation when implementing a control chart for monitoring the ratio $Z = X/Y$. In this paper, we tackle this problem by investigating the performance of the Phase II Shewhart-type RZ control chart monitoring the ratio of two normal variables whose relationship is captured by a bivariate time series autoregressive model VAR(1), which can also account for the cross-correlation between the two quality characteristics. With the numerical study, we discuss how the design and the statistical performance of the Shewhart-type RZ control chart change with the VAR(1) model's parameters. We also provide an example to illustrate the use of the Shewhart-type RZ control chart with bivariate time series of observations in a furnace process.

KEYWORDS

Quality control; multivariate autoregressive model; control charts

1. Introduction

In industrial manufacturing practice, control charts are a powerful tool to reduce variability and achieve process stability. Many control charts have been designed in Statistical Process Monitoring (SPM) literature to monitor the stability of many parameters characterizing the distribution of a quality characteristic like the Mean, the Median, the Standard Deviation, and the Coefficient of Variation (CV) (see for ex-

CONTACT Kim Duc Tran Email: ductk@donga.edu.vn

The contribution of the first author and the second author in the study are equal.

ample Amdouni et al. (2017), Faraz et al. (2018), and Mim et al. (2021)). The ratio between two normal random variables X and Y has been considered a quality characteristic to be monitored, as well. The reason is that the ratio can play an important role in ensuring the product quality of various processes. A number of situations where monitoring the ratio of two variables is useful have been listed as follows:

- **Food industry:** In this industry, the final product specifications may be related to the correct balance of nutrition associated with the relative weights of two ingredients within a food recipe. For such a process, the crucial quality characteristic to be monitored is the ratio of the mixture components.
- **Pharmaceutical industry:** In such industries, one of the crucial factors that ensures the safety and efficacy of drugs is the correct proportion ratio among active ingredients. In order to monitor product quality, this ratio can be measured before and after a chemical or physical reaction through an efficient control chart.
- **Industrial production:** In the industrial production of materials, raw elements are blended together into an alloy according to reciprocally optimized proportions in order to achieve some desired physical and chemical properties. Alternatively, it can represent a chemical or physical property of the product, which is defined as a ratio. As an example, in the diaper production industry, a critical quality characteristic is the speed of absorption $SA = \frac{Q}{t}$, computed by measuring the time $t[s]$ required for all the nominal quantity $Q[ml]$ of a saline solution to penetrate the diaper. Both Q and t are affected by random variability and can be considered as normal variables.
- **Energy management:** Another emerging field of an application would be on-line monitoring of yield Key Performance Indexes, defined as ratios between a consumed input and a process output: a typical example of an application could be the on-line monitoring of energy KPIs for continuous processes in energy management of industrial assets, which are expressed as daily ratios between the process output volume and the asset-by-asset consumed energy to get it.

Other examples related to the need of monitoring the ratio can be found in Spisak (1990) and Davis and Woodall (1991), from an unemployment insurance quality control program, or Oksoy et al. (1993) from on-line monitoring implemented in the glass industry.

The statistical properties of a Shewhart-RZ control chart have been presented in Celano et al. (2014) for individual measurements, (i.e by assuming the sample size $n = 1$), and Celano and Castagliola (2016a) for multiple measurements, (i.e when the sample size $n > 1$). Then, other advanced control charts have been proposed, such as the Synthetic-RZ control chart (Celano and Castagliola (2016b)), 4-out-of-5 runs rules-RZ control chart (Tran (2016)), the Run Rules-RZ control chart (Tran et al. (2016a)), the EWMA-RZ (Exponentially Weighted Moving Average) control chart (Tran et al. (2016b)), the CUSUM-RZ (Cumulative Sum) control chart (Tran et al. (2018)), the VSI EWMA-RZ (Variable Sampling Interval) control chart (Nguyen et al. (2019)), and the Short-Run Shewhart-RZ control chart (Tran et al. (2021)). Also, the effect of the measurement error on the ratio control chart has been investigated in Tran et al. (2016c) by using a linear covariate error model. The authors showed that the performance of this control chart can be significantly affected by the presence of measurement errors.

All the investigated RZ control charts in the literature have been designed under

the assumption that the observations collected for the two quality characteristics X and Y are independent. This assumption overlooks the problem of autocorrelation among consecutive observations, which is very frequent when measures of each quality characteristic are collected at a high rate, thus representing time series with a potentially high degree of autocorrelation. Modeling the consecutive observations as time series is then very important in SPM to avoid negative effects on the performance of the control chart monitoring the process. This is also a practical problem in smart manufacturing nowadays as the processes are mostly online monitoring. The data are real-time collected thanks to the wide use of sensors and IIoT (Industrial Internet of Things) technology. As a result, the independence assumption is regularly violated (Romoli and Lutey (2019); Alshraideh et al. (2020); Zhoua et al. (2021)). In SPM literature, many studies concerning the performance of various control charts in the presence of autocorrelation as well as the methods cope with have been proposed: see the review from Knoth and Schmid (2004) discussing papers related to the topic up to the beginning of the 2000s. One of the most important studies was conducted by Alwan and Roberts (1988), who illustrated the statistical modelling and fitting of time-series effects and the application of standard control charts to monitor the process stability. Later, Kalgonda and Kulkarni (2004) showed that autocorrelation has a serious impact on the performance of conventional control charts for multivariate data. With reference to the online monitoring of multivariate time series of observations, Leoni et al. (2015a) studied the effect of the autocorrelation on the performance of the T^2 chart when the observations are described by a bivariate first-order vector autoregressive (VAR(1)) time series model. A synthetic chart to control bivariate processes with autocorrelated data was designed in Leoni et al. (2015b) based on the VAR(1) model. Developing control charts in the presence of multivariate autocorrelated observations based on the VAR(1) model has been investigated by many researchers, see for example Brian Hwang and Wang (2010), Leoni et al. (2016), and Huang et al. (2014).

As far as we know, up to now, the effect of autocorrelation on the design and the statistical performance of an RZ control chart for monitoring the ratio has not yet been considered in the SPM literature. More precisely, being motivated by the existing gap in the related literature as well as the real challenges faced by the manufacturers in the industry, the main contributions of this study to the SPM literature can be summarized as follows:

- Providing the required theoretical background and investigating the performance of the Phase II Shewhart-type RZ control chart for monitoring the ratio of two normal random variables X and Y that are modeled by means of a bivariate VAR(1) model.
- Extending the results for monitoring the means ratio when the correlation structure between the observations follows a general class of the VAR(p) model.
- Discussing the issues to be considered by practitioners to design and implement the Shewhart-type RZ control chart.
- Showing the implementation of the MTS package within the R software environment for practitioners who want to run the Shewhart-RZ chart in real problems.

In summary, the main objective of this paper is to provide quality practitioners with a tool able to perform online monitoring of the ratio with high-frequency data collection, a condition that is rapidly spreading in the industry thanks to the evolution of sensor technologies.

Table 1. Summarized literature of the ratio and SPM applied to time series models.

Paper	Control chart	Within sample observations		Type of shifts	Time series model
		Independent	Autocorrelated		
Ratio chart ↓					
Celano et al. (2014)	Shewhart-RZ chart	✓		✓	
Tran (2016)	4-out-of-5 runs rules-RZ chart	✓		✓	
Celano and Castagliola (2016a)	Shewhart-RZ chart	✓		✓	
Celano and Castagliola (2016b)	Synthetic-RZ chart	✓		✓	
Tran et al. (2016a)	Run Rules-RZ chart	✓		✓	
Tran et al. (2016b)	EWMA-RZ chart	✓		✓	
Tran et al. (2016c)	RZ chart with measurement errors	✓		✓	
Tran et al. (2018)	CUSUM-RZ chart	✓		✓	
Nguyen et al. (2019)	VSI EWMA-RZ chart	✓		✓	
Tran et al. (2021)	Short-Run Shewhart-RZ chart	✓		✓	
SPM applied to time series ↓					
Kalgonda and Kulkarni (2004)	Z chart		✓	✓	✓
Brian Hwang and Wang (2010)	Neural-Network Identifier chart		✓	✓	✓
Leoni et al. (2015a)	Hotteling's T^2 chart		✓	✓	✓
Leoni et al. (2015b)	Hotteling's T^2 chart		✓	✓	✓
Leoni et al. (2016)	Hotteling's T^2 chart		✓	✓	✓
Present paper →	Shewhart-RZ		✓	✓	✓

Moreover, to show the main similarities and differences between the present study and some of the main related existing studies regarding the Ratio RZ chart and SPM methods applied to time series models, Table 1 is presented. In this table, the papers are summarized and categorized in terms of the control chart's scheme, presence or absence of autocorrelation within the sample observations, types of shifts in the quality parameter in terms of predicted (known) and random (unknown) shifts, the considered time series model when the within sample observations are assumed to be autocorrelated and following a VAR(1) model, a reduced VAR(1) model (the coefficient matrix is considered to be diagonal), or a VAR(p) model .

The paper is organized as follows: in Section 2, the distribution of the ratio Z is briefly recalled. In Section 3 the multivariate autoregressive model is presented for the special case of a bivariate time series. In Section 4, the formulas for the control limits and the performance metrics of the Shewhart-RZ control chart are discussed; in Section 5, the effect of the autocorrelation on the Shewhart-RZ control chart's performance is investigated; in Section 6, an illustrative example is provided to show how the Shewhart-RZ control chart should be run in presence of autocorrelation; some concluding remarks and recommendations for future research are given in Section 7. Finally, the mathematical results used in the study have been provided in the Appendices.

2. The ratio Z distribution

Let $\mathbf{W} = (X, Y)^T$ be a bivariate normal random vector of two quality characteristics X and Y , with mean vector $\boldsymbol{\mu}_{\mathbf{W}}$ and variance-covariance matrix $\boldsymbol{\Sigma}_{\mathbf{W}}$, where

$$\boldsymbol{\mu}_{\mathbf{W}} = \begin{pmatrix} \mu_X \\ \mu_Y \end{pmatrix}$$

and

$$\boldsymbol{\Sigma}_{\mathbf{W}} = \begin{pmatrix} \sigma_X^2 & \rho\sigma_X\sigma_Y \\ \rho\sigma_X\sigma_Y & \sigma_Y^2 \end{pmatrix},$$

where σ_X and σ_Y are the standard deviations of the two random variables X and Y of \mathbf{W} ; $\rho \in (-1, 1)$ is the coefficient of correlation. The ratio Z between the two components of \mathbf{W} , i.e. the quality characteristics X and Y , represents the ratio of two normal variables and is defined as $Z = \frac{X}{Y}$. Several studies on the distribution of this ratio have been published in the literature, see for example Hayya et al. (1975). Let $\gamma_X = \frac{\sigma_X}{\mu_X}$ and $\gamma_Y = \frac{\sigma_Y}{\mu_Y}$ be the coefficients of variation of X and Y , respectively, and let $\omega = \frac{\sigma_X}{\sigma_Y}$ be their standard-deviation ratio. In this study, to get the ratio distribution we apply an approximation for the inverse density function (*i.d.f*) $F_Z^{-1}(p|\gamma_X, \gamma_Y, \omega, \rho)$ of Z proposed by Celano and Castagliola (2016a) as

$$F_Z^{-1}(p|\gamma_X, \gamma_Y, \omega, \rho) \simeq \begin{cases} \frac{-C_2 - \sqrt{C_2^2 - 4C_1C_3}}{2C_1} & \text{if } p \in (0, 0.5], \\ \frac{-C_2 + \sqrt{C_2^2 - 4C_1C_3}}{2C_1} & \text{if } p \in [0.5, 1), \end{cases} \quad (1)$$

where C_1 , C_2 and C_3 are functions of p , γ_X , γ_Y , ω , and ρ , i.e.

$$\begin{aligned} C_1 &= \frac{1}{\gamma_Y^2} - (\Phi^{-1}(p))^2, \\ C_2 &= 2\omega \left(\rho(\Phi^{-1}(p))^2 - \frac{1}{\gamma_X\gamma_Y} \right), \\ C_3 &= \omega^2 \left(\frac{1}{\gamma_X^2} - (\Phi^{-1}(p))^2 \right). \end{aligned}$$

In this paper, like in Celano and Castagliola (2016a), we will assume that the coefficients of variations γ_X and γ_Y are typically in the range $(0, 0.2]$: in fact, small values of the coefficient of variation are desired in the quality control of a process, to maintain the process's inherent variability as small as possible to ensure output consistency. In this range, the above approximation has been found to be accurate (see Tran (2016)). Although in the existing literature on the RZ charts the consecutive couple observations (X_t, Y_t) are considered independent random variables, nevertheless they can be both autocorrelated and cross-correlated due to the velocity of data available in modern industrial processes.

3. The Vector Autoregressive VAR(1) model

The vector autoregressive VAR(1) model is one of the commonly used models to fit multivariate time series observations. Here, we consider the bivariate case, where two time series (i.e., the autocorrelated quality characteristics) X_t and Y_t can be modeled by a VAR(1) model. With this model for bivariate time series, each quality characteristic observation at time t not only linearly depends on the observation at time $t-1$ (autocorrelation), but it can also be linearly dependent on the observation of the other variable collected at time $t-1$, (cross-correlation). According to the VAR(1) model, the vector of the observations of the two quality characteristics at time t , say $\mathbf{W}_t = (X_t, Y_t)^\top$, depends on \mathbf{W}_{t-1} through the following equation

$$\mathbf{W}_t = \boldsymbol{\mu}_{\mathbf{W}} + \boldsymbol{\Phi}(\mathbf{W}_{t-1} - \boldsymbol{\mu}_{\mathbf{W}}) + \boldsymbol{\varepsilon}_t, \quad (2)$$

where

$$\boldsymbol{\mu}_{\mathbf{W}} = \begin{pmatrix} \mu_X \\ \mu_Y \end{pmatrix}$$

is the mean vector of \mathbf{W}_t ,

$$\boldsymbol{\Phi} = \begin{pmatrix} \Phi_{XX} & \Phi_{XY} \\ \Phi_{YX} & \Phi_{YY} \end{pmatrix}$$

is a (2×2) correlation matrix that accounts for both autocorrelation, (Φ_{XX} and Φ_{YY}), and cross-correlation, (Φ_{XY} and Φ_{YX}), between X and Y ; $\boldsymbol{\varepsilon}_t$ is the bivariate normal random noise with mean vector $\boldsymbol{\mu}_{\boldsymbol{\varepsilon}} = \mathbf{0}$ and variance-covariance matrix

$$\boldsymbol{\Sigma}_{\boldsymbol{\varepsilon}} = \begin{pmatrix} \sigma_{eX}^2 & \sigma_{eXY} \\ \sigma_{eXY} & \sigma_{eY}^2 \end{pmatrix}.$$

By these notations, eqn. (2) can also be rewritten as the following system of two equations

$$\begin{aligned} X_t &= \mu_X + \Phi_{XX}(X_{t-1} - \mu_X) + \Phi_{XY}(Y_{t-1} - \mu_Y) + \epsilon_{Xt} \\ Y_t &= \mu_Y + \Phi_{YX}(X_{t-1} - \mu_X) + \Phi_{YY}(Y_{t-1} - \mu_Y) + \epsilon_{Yt}. \end{aligned}$$

Based on the above equations, Φ_{XY} shows the linear dependence of X_t on Y_{t-1} in the presence of X_{t-1} . Φ_{YX} can also be interpreted in the same way. Hence, the univariate time series X_t and Y_t are not cross-correlated if $\Phi_{XY} = \Phi_{YX} = 0$. From (2), Reinsel (2003) showed that the variance-covariance matrix $\Sigma_{\mathbf{W}}$ of \mathbf{W}_t is the solution to the equation $\Sigma_{\mathbf{W}} = \Phi \Sigma_{\mathbf{W}} \Phi^\top + \Sigma_\epsilon$. Then, it can be shown that

$$\text{Vec}(\Sigma_{\mathbf{W}}) = (\mathbf{I}_4 - \Phi \otimes \Phi)^{-1} \text{Vec}(\Sigma_\epsilon), \quad (3)$$

where \mathbf{I}_4 is the 4×4 identity matrix, \otimes is the Kronecker product and Vec is the operator that transforms a matrix into a one-column vector by stacking its columns. Using (3), the variance-covariance matrix of the VAR(1) model in (2) can be obtained as

$$\begin{aligned} \Sigma_{\mathbf{W}} &= \begin{pmatrix} \sigma_X^2 & \rho\sigma_X\sigma_Y \\ \rho\sigma_X\sigma_Y & \sigma_Y^2 \end{pmatrix} \\ &= \begin{pmatrix} \frac{\Delta_{11}\sigma_{\epsilon_X}^2 + (\Delta_{12} + \Delta_{13})\sigma_{\epsilon_{XY}} + \Delta_{14}\sigma_{\epsilon_Y}^2}{\Delta} & \frac{\Delta_{31}\sigma_{\epsilon_X}^2 + (\Delta_{32} + \Delta_{33})\sigma_{\epsilon_{XY}} + \Delta_{34}\sigma_{\epsilon_Y}^2}{\Delta} \\ \frac{\Delta_{21}\sigma_{\epsilon_X}^2 + (\Delta_{22} + \Delta_{23})\sigma_{\epsilon_{XY}} + \Delta_{24}\sigma_{\epsilon_Y}^2}{\Delta} & \frac{\Delta_{41}\sigma_{\epsilon_X}^2 + (\Delta_{42} + \Delta_{43})\sigma_{\epsilon_{XY}} + \Delta_{44}\sigma_{\epsilon_Y}^2}{\Delta} \end{pmatrix}, \quad (4) \end{aligned}$$

where the quantities Δ_{sk} for $s, k = 1, 2, 3, 4$ are given in Appendix A.

In the next section, the sample means ratio $\bar{Z}_i = \frac{\bar{X}_i}{\bar{Y}_i}$ is suggested as the monitoring statistic of the Shewhart-type RZ control chart. Given the inverse distribution function of \bar{Z}_i in (1), one needs to get the distribution of the sample means vector $\bar{\mathbf{W}}_i = (\bar{X}_i, \bar{Y}_i)$ to calculate the control limits. It is proven in Appendix B that $\boldsymbol{\mu}_{\bar{\mathbf{W}}} = \boldsymbol{\mu}_{\mathbf{W}} = (\mu_X, \mu_Y)^\top$ and

$$\begin{aligned} \Sigma_{\bar{\mathbf{W}}} &= \begin{bmatrix} \sigma_{\bar{X}}^2 & \bar{\rho}\sigma_{\bar{X}}\sigma_{\bar{Y}} \\ \bar{\rho}\sigma_{\bar{X}}\sigma_{\bar{Y}} & \sigma_{\bar{Y}}^2 \end{bmatrix} \\ &= \frac{1}{n} \left[\Sigma_{\mathbf{W}} \left(\mathbf{I}_2 + \Lambda(\Phi^\top) - \frac{1}{n} \Pi(\Phi^\top) \right) + \left(\Lambda(\Phi) - \frac{1}{n} \Pi(\Phi) \right) \Sigma_{\mathbf{W}}^\top \right], \quad (5) \end{aligned}$$

where

$$\begin{aligned} \Lambda(\Phi) &= (\Phi - \Phi^n)(\mathbf{I}_2 - \Phi)^{-1} \\ \Pi(\Phi) &= (\Phi^{-1} - \mathbf{I}_2)^{-1} \left((\mathbf{I}_2 - \Phi^{n-1})(\mathbf{I}_2 - \Phi)^{-1} - (n-1)\Phi^{n-1} \right). \end{aligned}$$

In practice, the VAR(1) model parameters $\boldsymbol{\mu}$, Φ , and Σ_ϵ should be estimated from the Phase I observations. Several methods have been presented in the literature to obtain these estimated parameters such as the least squares (LS), maximum likelihood (ML), and Bayesian methods. Tsay (2013) (Chapt. 2) provided a detailed discussion about the theoretical aspects of these estimation methods and studied

their key properties. They showed that the Bayesian and LS methods produce close estimates, and under some conditions, the ML estimates are asymptotically equivalent to the LS ones. They also wrote several R functions included in the MTS package available in R (see Tsay and Wood (2018)) for multivariate time series analysis. Other statistical software such as SAS with the ARIMA procedure, can also be used to perform estimation of VAR models.

4. The implementation of the Shewhart-type RZ control chart with VAR(1) observations

Let us consider a process where a practitioner wants to monitor the ratio between two autocorrelated, and possibly cross-correlated, quality characteristics X and Y . At each inspection, n observations $(X_{i,j}, Y_{i,j})$, for $i = 1, \dots$, and $j = 1, \dots, n$ are collected. Similar to Tran et al. (2016a), we suggest monitoring the ratio \bar{Z}_i statistic defined as follows

$$\bar{Z}_i = \frac{\bar{X}_i}{\bar{Y}_i} = \frac{\frac{1}{n} \sum_{j=1}^n X_{i,j}}{\frac{1}{n} \sum_{j=1}^n Y_{i,j}} \quad (6)$$

at each time $i = 1, 2, \dots$. Let $\rho = \rho_0$ and $z = \frac{\mu_X}{\mu_Y} = z_0$ denote the coefficient of correlation between the two normal variables X and Y and the mean ratio when the process is in-control, respectively. As in the design of any control chart, the Shewhart-RZ chart for autocorrelated data is designed by defining its control limits. It is well-known that the distribution of the ratio of two normal random variables has no moment. Thus, the control limits of the Shewhart-RZ control chart monitoring \bar{Z}_i should be defined as probability control limits. Denoting as α the desired false alarm rate (FAR) for the control chart, the lower control limit (LCL) and the upper control limit (UCL) of the Shewhart-RZ are obtained from eqn. (1) as follows

$$LCL = F_Z^{-1} \left(\frac{\alpha}{2} \mid \gamma_{\bar{X}}, \gamma_{\bar{Y}}, \bar{\omega}, \bar{\rho} \right), \quad (7)$$

$$UCL = F_Z^{-1} \left(1 - \frac{\alpha}{2} \mid \gamma_{\bar{X}}, \gamma_{\bar{Y}}, \bar{\omega}, \bar{\rho} \right), \quad (8)$$

where $\gamma_{\bar{X}}$, $\gamma_{\bar{Y}}$, $\bar{\omega}$, and $\bar{\rho}$ should be computed from the mean vector $\boldsymbol{\mu}_{\bar{\mathbf{W}}}$ and the variance-covariance matrix $\boldsymbol{\Sigma}_{\bar{\mathbf{W}}}$ of the distribution of the bivariate sample mean vector $\bar{\mathbf{W}}_i = (\bar{X}_i, \bar{Y}_i)$ given in (5). Thus, to obtain LCL and UCL in (7) and (8), one can calculate the coefficients of variations $\gamma_{\bar{X}}$ and $\gamma_{\bar{Y}}$, the coefficient of correlation $\bar{\rho}$ between \bar{X}_i and \bar{Y}_i , and the standard-deviation ratio $\bar{\omega}$ as

$$\gamma_{\bar{X}} = \frac{\sigma_{\bar{X}}}{\mu_X}, \quad \gamma_{\bar{Y}} = \frac{\sigma_{\bar{Y}}}{\mu_Y}, \quad \bar{\rho} = \frac{\sigma_{\bar{X}, \bar{Y}}}{\sigma_{\bar{X}} \sigma_{\bar{Y}}}, \quad \bar{\omega} = \frac{\sigma_{\bar{X}}}{\sigma_{\bar{Y}}}, \quad (9)$$

respectively. Here, we assume that the coefficient of variation remains constant for each variable X and Y , i.e., $\sigma_{e_{X,i}} = \gamma_X \mu_{X,i}$ and $\sigma_{e_{Y,i}} = \gamma_Y \mu_{Y,i}$ for every $i \geq 1$. This implies that the standard deviation of each sample changes proportionally to its mean. There are several quality characteristics in practice (such as weights, tensile strengths and linear dimensions) that have a dispersion proportional to the population mean.

Thus, if we define $z = \frac{\mu_X}{\mu_Y} = z_0$, then the in-control ratio $\bar{\omega}$ can also be rewritten as

$$\bar{\omega} = \frac{\gamma_{\bar{X}}}{\gamma_{\bar{Y}}} \times \frac{\mu_X}{\mu_Y} = \frac{\gamma_{\bar{X}}}{\gamma_{\bar{Y}}} \times z_0. \quad (10)$$

When the process runs in the out-of-control state, the in-control ratio z_0 is shifted to $z_1 = \tau \times z_0$, where $\tau > 0$ is the shift size, and the in-control coefficient of correlation $\rho = \rho_0$ is shifted to $\rho = \rho_1$. According to the discussion in Leoni et al. (2015a), we can assume that the units within a sample are collected close together in time and, at the same time, the length h of the sampling interval is large enough to eliminate any dependence between successive values of the sample ratio statistics $\bar{Z}_1, \bar{Z}_2, \dots$. That is to say, the observations in each subgroup of size n follow a VAR(1) model but the ratio statistics $Z_i, i = 1, 2, \dots$ are independent random variables. Under the assumption of known (or perfect estimation of) distribution parameters, the run length of the Shewhart-RZ control chart follows a geometric distribution with a probability of *success* $p = 1 - \beta$, where

$$\beta = F_Z(UCL | \gamma_{\bar{X}}, \gamma_{\bar{Y}}, \bar{\omega}, \bar{\rho}) - F_Z(LCL | \gamma_{\bar{X}}, \gamma_{\bar{Y}}, \bar{\omega}, \bar{\rho}), \quad (11)$$

denotes the probability of that at any inspection following the occurrence of the assignable cause the control chart does not trigger any signal. The out-of-control parameters $\gamma_{\bar{X}}, \gamma_{\bar{Y}}, \bar{\omega}, \bar{\rho}$ in (11) can be calculated based on equation (9) or equations (14)–(17) but with $\rho = \rho_1$ and $z = z_1$. Then, the out-of-control average run length (ARL_1) and the out-of-control standard deviation run length ($SDRL_1$) of the Shewhart-RZ chart are computed as

$$\begin{aligned} ARL_1 &= \frac{1}{1 - \beta} \\ SDRL_1 &= \frac{\sqrt{\beta}}{1 - \beta}. \end{aligned} \quad (12)$$

Consider a case where X and Y are not cross-correlated and the matrix Φ is diagonal, i.e. $\Phi_{XY} = \Phi_{YX} = 0$, we aim to provide easier-to-use mathematical formulas for $\Sigma_{\mathbf{W}}, \Sigma_{\bar{\mathbf{W}}}, \gamma_{\bar{X}}, \gamma_{\bar{Y}}, \bar{\rho}$, and $\bar{\omega}$ when $n > 1$ observations are collected within each sample. The new results are helpful for practitioners to avoid time-consuming computations in the absence of cross-correlation. There are many examples in the SPM literature where the observations of one variable at a time $i, i = 2, 3, \dots$ are not dependent on the observations of the other variable at time $i - 1$, see for example Leoni et al. (2015a). As proved in Leoni et al. (2015a), if $\Phi_{XY} = \Phi_{YX} = 0$, then using (3), the variance-covariance matrix $\Sigma_{\mathbf{W}}$ of \mathbf{W}_i is equal to

$$\begin{aligned} \Sigma_{\mathbf{W}} &= \begin{pmatrix} \sigma_X^2 & \sigma_{XY} \\ \sigma_{XY} & \sigma_Y^2 \end{pmatrix} \\ &= \begin{pmatrix} (1 - \Phi_{XX}^2)^{-1} \sigma_{eX}^2 & (1 - \Phi_{XX} \Phi_{YY})^{-1} \sigma_{eXY} \\ (1 - \Phi_{XX} \Phi_{YY})^{-1} \sigma_{eXY} & (1 - \Phi_{YY}^2)^{-1} \sigma_{eY}^2 \end{pmatrix}. \end{aligned} \quad (13)$$

At time $i = 1, 2, \dots$, the sample mean vector $\bar{\mathbf{W}}_i = (\bar{X}_i, \bar{Y}_i)$ is also a bivariate

normal random vector with mean vector $\boldsymbol{\mu}_{\mathbf{W}}$ and variance-covariance matrix

$$\boldsymbol{\Sigma}_{\mathbf{W}} = \begin{pmatrix} \sigma_{\bar{X}}^2 & \bar{\rho}\sigma_{\bar{X}}\sigma_{\bar{Y}} \\ \bar{\rho}\sigma_{\bar{X}}\sigma_{\bar{Y}} & \sigma_{\bar{Y}}^2 \end{pmatrix},$$

where

$$\begin{aligned} \sigma_{\bar{X}}^2 &= \frac{\sigma_{e_X}^2}{n(1 - \Phi_{XX}^2)} \left(1 + \frac{2}{n} \sum_{k=1}^{n-1} (n-k) \Phi_{XX}^k \right), \\ \sigma_{\bar{Y}}^2 &= \frac{\sigma_{e_Y}^2}{n(1 - \Phi_{YY}^2)} \left(1 + \frac{2}{n} \sum_{k=1}^{n-1} (n-k) \Phi_{YY}^k \right), \\ \bar{\rho}\sigma_{\bar{X}}\sigma_{\bar{Y}} &= \frac{\rho\sigma_{e_X}\sigma_{e_Y}}{n(1 - \Phi_{XX}\Phi_{YY})} \left(1 + \frac{1}{n} \sum_{k=1}^{n-1} (n-k) \Phi_{XX}^k + \frac{1}{n} \sum_{k=1}^{n-1} (n-k) \Phi_{YY}^k \right). \end{aligned}$$

From these quantities, it is straightforward to obtain the coefficients of variations $\gamma_{\bar{X}} = \frac{\sigma_{\bar{X}}}{\mu_X}$ and $\gamma_{\bar{Y}} = \frac{\sigma_{\bar{Y}}}{\mu_Y}$ of \bar{X}_i and \bar{Y}_i as

$$\gamma_{\bar{X}} = \frac{\sigma_{e_X} \sqrt{1 + \frac{2}{n} \sum_{k=1}^{n-1} (n-k) \Phi_{XX}^k}}{\sqrt{n(1 - \Phi_{XX}^2)} \mu_X} \quad (14)$$

$$\gamma_{\bar{Y}} = \frac{\sigma_{e_Y} \sqrt{1 + \frac{2}{n} \sum_{k=1}^{n-1} (n-k) \Phi_{YY}^k}}{\sqrt{n(1 - \Phi_{YY}^2)} \mu_Y}. \quad (15)$$

Similarly, the coefficient of correlation $\bar{\rho}$ between \bar{X}_i and \bar{Y}_i is defined as

$$\bar{\rho} = \frac{\rho \sqrt{(1 - \Phi_{XX}^2)(1 - \Phi_{YY}^2)} \left(1 + \frac{1}{n} \sum_{k=1}^{n-1} (n-k) \Phi_{XX}^k + \frac{1}{n} \sum_{k=1}^{n-1} (n-k) \Phi_{YY}^k \right)}{(1 - \Phi_{XX}\Phi_{YY}) \sqrt{\left(1 + \frac{2}{n} \sum_{k=1}^{n-1} (n-k) \Phi_{XX}^k \right) \left(1 + \frac{2}{n} \sum_{k=1}^{n-1} (n-k) \Phi_{YY}^k \right)}}, \quad (16)$$

and the standard-deviation ratio $\bar{\omega} = \frac{\sigma_{\bar{X}}}{\sigma_{\bar{Y}}}$ is

$$\bar{\omega} = \frac{\sigma_{e_X} \sqrt{(1 - \Phi_{YY}^2)}}{\sigma_{e_Y} \sqrt{(1 - \Phi_{XX}^2)}} \times \sqrt{\frac{1 + \frac{2}{n} \sum_{k=1}^{n-1} (n-k) \Phi_{XX}^k}{1 + \frac{2}{n} \sum_{k=1}^{n-1} (n-k) \Phi_{YY}^k}}.$$

Concerning $\bar{\omega}$, it is important to note that if we let $z = \frac{\mu_X}{\mu_Y}$, it can also be rewritten as

$$\bar{\omega} = \frac{\gamma_{\bar{X}}}{\gamma_{\bar{Y}}} \times \frac{\mu_X}{\mu_Y} = \frac{\gamma_{\bar{X}}}{\gamma_{\bar{Y}}} \times z. \quad (17)$$

Now, the *LCL* and *UCL* in (7) and (8) can be recalculated based on equations (14)-(17). Finally, we summarize all the needed steps to estimate the control limits of the Shewhart-RZ control chart and implement it to perform online monitoring.

- Phase I. Retrospective study.

- Step 1 Select a Phase I sample of size m (for example $m = 100$ observations of the two quality characteristics X and Y) to carry out a process stability study.
- Step 2 Perform a multivariate time series study on the individual (X_t, Y_t) observations for $t = 1, \dots, m$ to check that the VAR(1) is a suitable time series model based on the investigation of the sample ACF (autocorrelation function), PACF (partial autocorrelation function), and CCF (cross-correlation function).
- Step 3 Estimate the VAR(1) parameters with the function `VAR` in the MTS package available within the R software environment.
- Step 4 Check the normality of the residuals using a normal probability plot and an Anderson Darling test.
- Step 5 Investigate the stability of the residuals by using a bivariate control chart for individual observations.
- Step 6 Set a sample size n such that the ratios are uncorrelated, even if the observations within each sample are VAR(1). The decision about the sample size is based on the sample ACF and PACF investigation for Phase I ratios obtained with different values of n .
- Step 7 Calculate the elements $\gamma_{\bar{X}}, \gamma_{\bar{Y}}, \bar{\rho}$, and $\bar{\omega}$ of $F_Z^{-1}(\cdot)$ based on eqns. (9) and (10) if Φ_{XY} and/or Φ_{YX} are non-zero, and based on eqns. (14)-(17) if $\Phi_{XY} = \Phi_{YX} = 0$.
- Step 8 Set a target in-control average run length ARL_0 (for example $ARL_0 = 200$) and calculate $\alpha = \frac{1}{ARL_0}$.
- Step 9 Compute the control limits (LCL, UCL) from eqns. (7) and (8).
- Step 10 Split the Phase I sample into s samples of size n such that $m = s * n$ and calculate the sample means \bar{X}_i and \bar{Y}_i and then the sample ratios \bar{Z}_i for each sample $i = 1, 2, \dots, s$.
- Step 11 Plot the sample ratios \bar{Z}_i on the control chart.
- Step 12 If $LCL \leq \bar{Z}_i \leq UCL$ for all i , i.e., the Phase I dataset is stable, fix the control limits LCL and UCL and go to Phase II. Otherwise, if there are some out-of-control signals, remove the samples related to the signal conditions from the Phase I dataset and repeat Steps 2-12.
- Phase II. On-line monitoring.
- Step 1 Consider the following input data:
- A sample size n (for example $n = 5$).
 - A target ARL_0 and $\alpha = \frac{1}{ARL_0}$ (for example $ARL_0 = 200$ and then $\alpha = 0.05$).
 - The estimated VAR(1) model parameters $(\boldsymbol{\mu}_{\overline{\mathbf{W}}}, \boldsymbol{\Phi}, \boldsymbol{\Sigma}_\epsilon, \boldsymbol{\Sigma}_{\overline{\mathbf{W}}})$.
 - The calculated RZ distribution parameters $(\gamma_{\bar{X}}, \gamma_{\bar{Y}}, \bar{\rho}_0, \bar{\omega})$.
 - The obtained LCL and UCL during Phase I.
- Step 2 Collect n observations at each inspection.
- Step 3 Calculate the sample means \bar{X}_i and \bar{Y}_i and the sample ratios \bar{Z}_i for each sample $i = 1, 2, \dots$.
- Step 4 Declare an out-of-control signal if $\bar{Z}_i < LCL$ or $\bar{Z}_i > UCL$. Otherwise, continuous process monitoring.

Although with industrial data $p = 1$ in VAR(p) model is enough to account for the process inertia and consecutive observations autocorrelation, following Tsay(2013) and the results regarding the VAR(1) model, the computations of the Shewhart-RZ control chart for the VAR(p) model are also derived in Appendix C.

5. Numerical Study

In this Section, we present the effect of autocorrelation on the performance of the Shewhart-RZ control evaluated by using ARL and $SDRL$ metrics. The ARL_1 and $SDRL_1$ values are computed from (12) given the fixed values of parameters n , $\gamma_X = \frac{\sigma_{\varepsilon_X}}{\mu_X}$, $\gamma_Y = \frac{\sigma_{\varepsilon_Y}}{\mu_Y}$, Φ_{XX} , Φ_{YY} , z_0 , ρ_0 , ρ_1 , and τ . Without loss of generality, we assume that $z_0 = 1$. For the sake of brevity and clarity of discussion, we also suppose that X and Y are not cross-correlated and the matrix Φ is diagonal, i.e. $\Phi_{XY} = \Phi_{YX} = 0$. It allows reducing the bivariate stationary conditions to the more simple univariate stationary conditions for each variable and it has already been stated by Leoni et al. (2015a). Tables showing the cross-correlation effect on the control chart's design and performance are available upon request from the authors. The in-control ARL is set at $ARL_0 = 200$, corresponding to the FAR $\alpha = 0.005$. In this study, we also assume $n \in \{2, 5, 7, 10, 15\}$, $\gamma_X \in \{0.01, 0.2\}$, $\gamma_Y \in \{0.01, 0.2\}$, $\rho_0 \in \{-0.9, -0.4, 0, 0.4, 0.9\}$, and $\Phi_{XX}, \Phi_{YY} \in \{0.1, 0.7\}$.

The values of the control limits (LCL, UCL) of the Shewhart-RZ control chart for the case $\Phi_{XX} = \Phi_{YY} = 0.1$ are presented in Table 2. Results have also been obtained for other parameters but they are not presented here and are available upon request from the authors. Similar to the Shewhart-RZ control chart for independent observations investigated in Celano and Castagliola (2016a), it can be seen from this table that with the same value of sample size n , the values of LCL and UCL depend on both the value of ρ_0 , (given (γ_X, γ_Y)), and the value of (γ_X, γ_Y) , (given the value of ρ_0). The increase of ρ_0 leads to an increase of LCL and a decrease of UCL . For example, with $(\gamma_X, \gamma_Y) = (0.01, 0.01)$ and $n = 5$, we have $LCL = 0.9711$ and $UCL = 1.0297$ when $\rho_0 = -0.9$, compared to $LCL = 0.9837$ and $UCL = 1.0166$ when $\rho_0 = 0.4$. By contrast, the increase of (γ_X, γ_Y) leads to the decrease of LCL and the increase of UCL . For example, with $n = 7$ and $\rho_0 = 0.0$, we have $LCL = 0.9820$ and $UCL = 1.0184$ when $(\gamma_X, \gamma_Y) = (0.01, 0.01)$ compared to $LCL = 0.6878$ and $UCL = 1.4539$ when $(\gamma_X, \gamma_Y) = (0.2, 0.2)$.

INSERT TABLE 2 ABOUT HERE

We present the effect of the autocorrelation between observations on the Shewhart-RZ chart in Tables 3-6 assuming that the correlation coefficient ρ between the random variables X and Y does not be affected by the assignable causes, i.e. $\rho_0 = \rho_1$. In particular, Tables 3-4 show the values of ARL_1 and $SDRL_1$ corresponding to the case $\Phi_{XX} = \Phi_{YY}$ and Tables 5-6 show the values of ARL_1 and $SDRL_1$ when $\Phi_{XX} \neq \Phi_{YY}$. In general, the obtained results show that given the values of other parameters, the increase of Φ_{XX} or Φ_{YY} , or both of them leads to the increase of the ARL_1 and $SDRL_1$; the larger the values of (Φ_{XX}, Φ_{YY}) , the larger the values of the ARL_1 and $SDRL_1$. For example, in Table 3 for fixed values of $n = 5$, $(\gamma_X, \gamma_Y) = (0.01, 0.01)$, $\rho_0 = \rho_1 = -0.9$ and $\tau = 0.99$, we obtain $ARL_1 = 24.8$ and $SDRL_1 = 24.3$ when $(\Phi_{XX}, \Phi_{YY}) = (0.1, 0.1)$ compared to $ARL_1 = 97.9$ and $SDRL_1 = 97.4$ when $(\Phi_{XX}, \Phi_{YY}) = (0.7, 0.7)$. Both of these values are larger than the value $ARL_1 = 19.1$ and $SDRL_1 = 18.59$ when the process is free of autocorrelation (i.e. $(\Phi_{XX}, \Phi_{YY}) = (0, 0)$) as pointed out in Celano and Castagliola (2016a). That is to say, the autocorrelation between observations has a negative influence on the Shewhart-RZ's performance: it reduces the ability of the Shewhart-RZ control chart in detecting the process shift or out-of-control conditions.

INSERT TABLE 3 ABOUT HERE

INSERT TABLE 4 ABOUT HERE

INSERT TABLE 5 ABOUT HERE

INSERT TABLE 6 ABOUT HERE

We also consider the situation when the occurrence of an assignable cause shifts the correlation coefficient ρ from ρ_0 to ρ_1 . The values of ARL_1 and $SDRL_1$ corresponding to this situation are presented in Tables 7-8. For the brevity of the paper, we only show the ARL_1 values for the case $\Phi_{XX} = \Phi_{YY}$. The negative effect of autocorrelation on the chart's performance can also be seen in these two tables. Moreover, it is worth noting that when both the nominal ratio and the correlation coefficient are shifted, for the process with high values of (γ_X, γ_Y) , the Shewhart-RZ control chart is on average inefficient in detecting shifts as the values of ARL_1 are too large (see the case $(\gamma_X, \gamma_Y) = (0.2, 0.2)$ in Table 7).

INSERT TABLE 7 ABOUT HERE

INSERT TABLE 8 ABOUT HERE

In several cases when there is no preference for any specific shift size, one may suggest assigning a distribution for the process shift in a predicted interval. The expected average run length ($EARL$) is used to evaluate the statistical performance of the corresponding chart, where

$$EARL = \int_{\Omega} ARL \times f_{\tau}(\tau) d\tau, \quad (18)$$

in which $f_{\tau}(\tau)$ stands for the distribution of the shift size τ in the interval Ω and ARL is as defined in (12). When there is no information about τ , a uniform distribution of τ could be applied, i.e. we have $f_{\tau}(\tau) = \frac{1}{b-a}$ for $\tau \in \Omega = [a, b]$.

The effect of Φ_{XX} and Φ_{YY} on the overall performance of the Shewhart-RZ control chart in the presence of autocorrelation is displayed in Figure 1 ($\rho_0 = \rho_1 = -0.9$) and Figure 2 ($\rho_0 = -0.4$ and $\rho_1 = -0.9$) with the $EARL$ values for two possibilities of Ω , including $\Omega = \Omega_D = [0.9, 1)$ (decreasing case, denoted as (D)) and $\Omega = \Omega_I = (1, 1.1]$ (increasing case, denoted as (I)). We also consider several values of Φ_{XX} and Φ_{YY} as $\Phi_{XX} \in \{0.1, 0.2, \dots, 0.7\}$ and $\Phi_{YY} \in \{0.1, 0.2, \dots, 0.7\}$. The values of other parameters are presented in the caption of each figure. In general, the obtained values of $EARL$ in these figures show a similar trend of the negative effect of Φ_{XX} and Φ_{YY} (representing the autocorrelation between observations) on the overall performance of the Shewhart-RZ chart as the specific shift size cases. In most cases, the larger the values of (Φ_{XX}, Φ_{YY}) , the larger the values of $EARL$, namely the slower the Shewhart-RZ control chart in detecting the out-of-control conditions. For example, in Figure 1 with $n = 15$, $\Omega = [0.9, 1)$, $\rho_0 = \rho_1 = -0.9$, $\gamma_X = \gamma_Y = 0.01$, we have $EARL = 1.87$ for $\Phi_{XX} = \Phi_{YY} = 0.1$, $EARL = 4.71$ for $\Phi_{XX} = \Phi_{YY} = 0.5$, and $EARL = 6.52$ for $\Phi_{XX} = \Phi_{YY} = 0.7$. These values are all larger than $EARL = 1.4$ for $\Phi_{XX} = \Phi_{YY} = 0$ (the process is free of autocorrelation) as presented in Celano and Castagliola (2016a) (Table 6).

INSERT FIGURE 1 ABOUT HERE

INSERT FIGURE 2 ABOUT HERE

As mentioned earlier in Section 2, the method proposed by Celano and Castagliola (2016a) is used to calculate the control limits of the RZ chart based on the (approximated) inverse density function of the ratio Z . In what follows, the accuracy of the applied approximation is assessed, in particular in the presence of autocorrelation, through a simulation study. Although the exact analytical form of the inverse density function of the ratio Z is complicated to obtain, some helpful results can be derived using Monte-Carlo simulations. To this end, $B = 100,000$ samples are generated from a bivariate VAR(1) model with some specified parameters and sample sizes. Then, for each sample, the ratio \bar{Z} is calculated. The accuracy of the approximation is investigated with respect to the sample size n , the coefficients of variation γ_X and γ_Y , and the correlation coefficient ρ . It is worth mentioning that we have used the function `VARMAsim` of the MTS R package to generate VAR(1) observations. Figure 3 shows the empirical inverse density function of the ratio \bar{Z} obtained by simulation (continuous line) and its approximation (dashed line), as in Celano and Castagliola (2016a). The figure shows that while the sample size has the largest effect on the approximation, there is no significant difference between the empirical and exact inverse density function when the other parameters vary (see Figure 3). More precisely, the larger n the more accurate the approximation. From a practical point of view, sample sizes $n \geq 4$ can be used in practice to get an acceptable approximation (see Figure 3 (a)-(c)).

INSERT Figure 3 ABOUT HERE

As the last step of numerical analysis, let us assess the impact of overlooking the autocorrelation among the observations on the statistical performance of the Shewhart-type RZ. In the Introduction Section, it was mentioned that Celano and Castagliola (2016a) developed the Shewhart-RZ control chart with multiple measurements when there is no autocorrelation among the observations within each sample. In what follows, we investigate the effect of overlooking autocorrelation on the *ARL* performance of this chart. More precisely, we want to investigate how much the in-control performance changes if the quality inspector uses the control limits of the Shewhart-RZ control chart presented in Celano and Castagliola (2016a), while the observations within each sample follow a VAR(1) model. To this end, we conduct a numerical comparison by assessing the impact of autocorrelation parameters on the in-control *ARL* of the chart. The results of the comparison study for some combinations of Φ_{XX} , Φ_{YY} , ρ , γ_X , γ_Y , and n are presented in Table 9. The presented in-control *ARL* values in this table are obtained through simulations. From this table, it can be observed that the in-control performance of the chart is dramatically affected by the autocorrelation coefficients Φ_{XX} and Φ_{YY} and the sample size n . In particular, the in-control *ARL* strongly reduces when the coefficients Φ_{XX} and Φ_{YY} move from 0 to 1, thus leading to an excessive number of false alarms. For example, when $\Phi_{XX} = \Phi_{YY} = 0.7$, $\rho_0 = 0.9$, $\gamma_X = \gamma_Y = 0.2$ and $n = 15$, the actual in-control *ARL* of the chart is 5.03 while it is expected to be 200. The table also shows that for the same values of Φ_{XX} and Φ_{YY} , the in-control *ARL* decreases with n .

INSERT Table 9 ABOUT HERE

6. Illustrative example

In this Section, we provide an example to illustrate the implementation of the Shewhart-type RZ control charts with VAR(1) observations. In particular, we consider the bivariate time series dataset of $N=185$ individual observations ($n = 1$) of the measured pressure in psi at the front and back end of an industrial furnace recorded every ten minutes reported in Montgomery et al. (2015) (p. 347). Let us denote the front and back pressure as X and Y , respectively. Montgomery et al. (2015) studied the sample ACF and CCF plots and concluded that the individual time series X_i and Y_i , for $i = 1, \dots, 185$, are autocorrelated and cross-correlated with each other. They also proposed the VAR(1) model as an appropriate fit for the time series data. Here, we are going to analyze this dataset in an SPM setting by monitoring the ratio of pressures at the front and back of the furnace as the heating process quality characteristic of interest. Controlling the furnace pressure is essential to achieve a high heating process efficiency. In fact, when the pressure is too low, cold air can infiltrate, and burned gas tends to condensate, due to the excessive presence of air. This problem is critical in industrial furnaces, where the distance between the front end and back end can facilitate the occurrence of an uncontrolled pressure imbalance and, therefore, external air infiltration. To this end, let us have considered the first $m = 100$ individual observations as the Phase I dataset to estimate the model's parameters and plot the Phase I control chart and the remaining $m = 85$ individual observations for the online monitoring purpose (Phase II implementation of the control chart). We assume that the time series model parameters are perfectly estimated from the Phase I retrospective sample. The Phase I dataset is reported in Table 10.

INSERT TABLE 10 ABOUT HERE

INSERT Figure 4 ABOUT HERE

INSERT Figure 5 ABOUT HERE

We start from the Phase I dataset study to check the process stability. Figure 4 shows the plots of individual time series X_t and Y_t . The sample ACF and PACF plots of the given time series are given in Figures 5 (a-d). These figures demonstrate that in both cases an AR model seems to be suitable. Thus, assuming the VAR(1) model proposed by Montgomery et al. (2015) to fit the bivariate time series, to estimate the model's parameters, we have used the function `VAR` in the MTS R package that runs the least squares estimation method. From Table 10, it is easy to get $\hat{\boldsymbol{\mu}}_{\mathbf{W}} = \boldsymbol{\mu}_{\overline{\mathbf{W}}} = (\bar{X}, \bar{Y})^\top = (10.885, 20.363)^\top$. Combining the mean vector with the output of `VAR` function gives the following VAR(1) autoregressive model

$$\begin{pmatrix} X_{i,j} \\ Y_{i,j} \end{pmatrix} = \begin{pmatrix} 10.885 \\ 20.363 \end{pmatrix} + \begin{pmatrix} 0.663 & 0.464 \\ 0.434 & -0.551 \end{pmatrix} \left[\begin{pmatrix} X_{i,j-1} \\ Y_{i,j-1} \end{pmatrix} - \begin{pmatrix} 10.885 \\ 20.363 \end{pmatrix} \right] + \begin{pmatrix} \varepsilon_{j,X} \\ \varepsilon_{j,Y} \end{pmatrix} \quad (19)$$

where

$$\begin{pmatrix} \varepsilon_{j,X} \\ \varepsilon_{j,Y} \end{pmatrix} \sim N_2 \left(\mathbf{0}, \hat{\boldsymbol{\Sigma}}_{\boldsymbol{\varepsilon}} = \begin{pmatrix} 1.257 & 0.399 \\ 0.399 & 1.040 \end{pmatrix} \right). \quad (20)$$

In the next step, after estimating the VAR(1) model parameters, the quality practitioner should analyze the residuals. The probability plots in Figure 5 (e and f)

show that the residuals follow the normal distribution, as well as the cross-correlation plot of VAR(1) model residuals in Figure 5 (g), shows that there is no strong cross-correlation among residuals. By these results, one can check the VAR(1) residuals' stability with a Hotelling's T^2 chart, Figure 5 (h). From the control chart, it can be seen that the Phase I residuals are stable. Therefore, we can compute the parameters for the Phase I ratio distribution and the ratio statistics \bar{Z}_i .

INSERT Figure 6 ABOUT HERE

Now, a sample size n such that the ratios are uncorrelated should be selected, even if the observations (X_{ij}, Y_{ij}) for $j = 1, 2, \dots, n$ within each sample i are VAR(1). The decision about the sample size is based on the sample ACF and PACF study for the Phase I ratios obtained with different values of n . We assessed this issue and found that $n = 5$ is sufficient to eliminate autocorrelation for the ratios, even if the individual observations within each sample are VAR(1), see figure 6. Therefore, samples of $n = 5$ observations are collected, where the first one is collected at the beginning of each hour of production. From eqns. (4) and (5) and the fact that $n = 5$, we obtained

$$\hat{\Sigma}_{\mathbf{w}} = \begin{pmatrix} 3.978 & 0.897 \\ 0.897 & 1.953 \end{pmatrix} \quad (21)$$

$$\hat{\Sigma}_{\bar{\mathbf{w}}} = \begin{pmatrix} 2.855 & 0.949 \\ 0.949 & 0.418 \end{pmatrix} \quad (22)$$

To check the stability of the Phase I dataset, let the in-control ratio $z_0 = \frac{\mu_X}{\mu_Y} = \frac{10.885}{20.363} = 0.535$. In addition, the parameters of $F_Z^{-1}(\dots)$ in (1) can be calculated from equations (9) and (10):

$$\begin{aligned} \hat{\gamma}_{\bar{X}} &= \frac{\hat{\sigma}_{\bar{X}}}{\hat{\mu}_{\bar{X}}} = \frac{\sqrt{2.855}}{10.885} = 0.155, & \hat{\gamma}_{\bar{Y}} &= \frac{\hat{\sigma}_{\bar{Y}}}{\hat{\mu}_{\bar{Y}}} = \frac{\sqrt{0.418}}{20.363} = 0.032, \\ \hat{\rho} &= \frac{\hat{\sigma}_{\bar{X}\bar{Y}}}{\hat{\sigma}_{\bar{X}}\hat{\sigma}_{\bar{Y}}} = \frac{0.949}{\sqrt{2.855}\sqrt{0.418}} = 0.869, & \hat{\omega} &= \frac{\hat{\gamma}_{\bar{X}}}{\hat{\gamma}_{\bar{Y}}} \times z_0 = \frac{0.155}{0.032} \times 0.535 = 2.591. \end{aligned}$$

From (7)-(8), the control limits of the proposed Shewhart-RZ chart in this case are calculated as

$$\begin{aligned} LCL &= F_Z^{-1}(0.0025 | \hat{\gamma}_{\bar{X}} = 0.155, \hat{\gamma}_{\bar{Y}} = 0.032, \hat{\omega} = 2.591, \hat{\rho} = 0.869) \\ &= 0.327 \\ UCL &= F_Z^{-1}(0.9975 | \hat{\gamma}_{\bar{X}} = 0.155, \hat{\gamma}_{\bar{Y}} = 0.032, \hat{\omega} = 2.591, \hat{\rho} = 0.869) \\ &= 0.715. \end{aligned}$$

Figure 7 (a) shows the Shewhart-RZ control chart as well as the ratio statistics Z_i for Phase I observations based on samples #1 to #20 each of size $n = 5$. Since the control limits $LCL = 0.327$ and $UCL = 0.715$ does not trigger any out-of-control signal for Phase I observations, therefore, these control limits can be used for the Phase II implementation of the control chart.

The Phase II dataset is presented in Table 11 together with the corresponding sample means \bar{X}_i and \bar{Y}_i and the sample ratios \bar{Z}_i .

INSERT TABLE 11 ABOUT HERE

INSERT Figure 7 ABOUT HERE

Figure 7 (b) shows the Phase II control chart for samples #21 to #37. An assignable cause leads to a downward shift of the ratio z_0 between samples #30 and #33. This results in a too large pressure unbalance between the front and back end pressure moving air towards the furnace entrance, with consequent problems to the heating process of material conveyed within the chamber. The chart signals the occurrence of the out-of-control condition by plotting points #32 and #33 below the LCL (see also bold values in Table 11). An intervention on the furnace pressure sensors eliminates the assignable cause and brings the process back to the in-control condition. Finally, we warn readers that this example was worked with a relatively small benchmark dataset from Montgomery et al. (2015) to facilitate the reproduction of results. For this reason, we assumed a perfect estimation of time series parameters from the Phase I retrospective study. However, we remember to practitioners that collecting a dataset of VAR observations consisting of several hundred or thousands of observations can significantly improve the reliability of the time series parameters estimation. Therefore, we strongly encourage practitioners to cope with large retrospective samples, whenever they are available. In the Conclusion Section, we stress this issue as a further research direction.

7. Conclusions

In this paper, we have investigated the effects of autocorrelation on the performance of the Shewhart-RZ control chart using an autoregressive model for the sample ratio. The ARL , $SDRL$, and $EARL$ metrics are used to evaluate the performance of the Shewhart-RZ chart for the specific shift size (using ARL and $SDRL$) or the overall performance (using $EARL$). The obtained results show that the autocorrelation between observations has a negative impact on the Shewhart-RZ chart's performance. It reduces the ability of the chart in detecting process shifts compared to no autocorrelation case. The presented results also show that the Shewhart control chart is not efficient in detecting small shifts for the process with high values of coefficient of variation (i.e. γ_X, γ_Y). However, the following topics could be interesting directions for further research:

- Designing other advanced control charts to reduce the negative impact of the autocorrelation on the chart's performance.
- Investigating the effect of autocorrelation on the performance of the EWMA-RZ control chart along similar lines.
- Assessing the reliability of Phase I implementation for processes with autocorrelated observations on the RZ-type control charts is essential to its correct implementation. In particular, a thorough study of the dimension of the Phase I dataset (i.e. the retrospective sample) is important to assess the effect of past process knowledge available from automatic sensor readings. A good balance between the size of the retrospective study and the probability of having process shifts during the Phase I implementation should be carefully investigated.

Data Availability Statement

All data analyzed during this study are included in this paper.

References

- Alshraideh, H., Del Castillo, E., & Del Val, A. G. (2020). Process control via random forest classification of profile signals: An application to a tapping process. *Journal of Manufacturing Processes*, 58, 736-748.
- Alwan, L. C., & Roberts, H. V. (1988). Time-series modeling for statistical process control. *Journal of Business & Economic Statistics*, 6(1), 87-95.
- Amdouni, A., Castagliola, P., Taleb, H., & Celano, G. (2017). A variable sampling interval Shewhart control chart for monitoring the coefficient of variation in short production runs. *International Journal of Production Research*, 55(19), 5521-5536.
- Brian Hwang, H., & Wang, Y. (2010). Shift detection and source identification in multivariate autocorrelated processes. *International Journal of Production Research*, 48(3), 835-859.
- Celano, G., & Castagliola, P. (2016a). Design of a phase II control chart for monitoring the ratio of two normal variables. *Quality and Reliability Engineering International*, 32(1), 291-308.
- Celano, G., & Castagliola, P. (2016b). A synthetic control chart for monitoring the ratio of two normal variables. *Quality and Reliability Engineering International*, 32(2), 681-696.
- Celano, G., Castagliola, P., Faraz, A., & Fichera, S. (2014). Statistical performance of a control chart for individual observations monitoring the ratio of two normal variables. *Quality and Reliability Engineering International*, 30(8), 1361-1377.
- Davis, R. B., & Woodall, W. H. (1991). Evaluation of control charts for ratios. In *22nd Annual Pittsburgh Conference on Modeling and Simulation* (pp. 63-70).
- Faraz, A., Heuchenne, C., & Saniga, E. (2018). An exact method for designing Shewhart and S^2 control charts to guarantee in-control performance. *International Journal of Production Research*, 56(7), 2570-2584.
- Hayya, J., Armstrong, D., & Gressis, N. (1975). A note on the ratio of two normally distributed variables. *Management Science*, 21(11), 1338-1341.
- Huang, X., Bisgaard, S., & Xu, N. (2014). Model-based multivariate monitoring charts for autocorrelated processes. *Quality and Reliability Engineering International*, 30(4), 527-543.
- Hubbard, J. H., & Hubbard, B. B. (2015). *Vector Calculus, Linear Algebra, and Differential Forms: A Unified Approach* (pp. 818-pages). Matrix Editions.
- Kalgonda, A. A., & Kulkarni, S. R. (2004). Multivariate quality control chart for autocorrelated processes. *Journal of Applied Statistics*, 31(3), 317-327.
- Knoth, S., & Schmid, W. (2004). Control charts for time series: A review. *Frontiers in Statistical Quality Control*, 7, 210-236, Physica, Heidelberg.
- Leoni, R. C., Costa, A. F. B., Franco, B. C., & Machado, M. A. G. (2015b). The skipping strategy to reduce the effect of the autocorrelation on the T^2 chart's performance. *The International Journal of Advanced Manufacturing Technology*, 80(9), 1547-1559.
- Leoni, R. C., Costa, A. F. B., & Machado, M. A. G. (2015a). The effect of the autocorrelation on the performance of the T^2 chart. *European Journal of Operational Research*, 247(1), 155-165.
- Leoni, R. C., Machado, M. A. G., & Costa, A. F. B. (2016). The T^2 chart with mixed samples to control bivariate autocorrelated processes. *International Journal of Production Research*, 54(11), 3294-3310.
- Lütkepohl, H. (2005). *New Introduction to Multiple Time Series Analysis*. Springer Science & Business Media.
- Mim, F. N., Khoo, M. B., Saha, S., & Castagliola, P. (2021). Revised triple sampling control charts for the mean with known and estimated process parameters. *International Journal of Production Research*, 1-25. doi.org/10.1080/00207543.2021.1943035.

- Montgomery, D. C., Jennings, C. L., & Kulahci, M. (2015). *Introduction to Time Series Analysis and Forecasting*. John Wiley & Sons.
- Nguyen, H. D., Tran, K. P., & Heuchenne, C. (2019). Monitoring the ratio of two normal variables using variable sampling interval exponentially weighted moving average control charts. *Quality and Reliability Engineering International*, 35(1), 439-460.
- OKSOY, D., Boulos, E., & DAVID PYE, L. (1993). Statistical process control by the quotient of two correlated normal variables. *Quality Engineering*, 6(2), 179-194.
- Reinsel, G. C. (2003). *Elements of Multivariate Time Series Analysis*. Springer Science & Business Media.
- Romoli, L., & Lutey, A. H. A. (2019). Quality monitoring and control for drilling of CFRP laminates. *Journal of Manufacturing Processes*, 40, 16-26.
- Spisak, A. W. (1990). A control chart for ratios. *Journal of Quality Technology*, 22(1), 34-37.
- Tran, K. P. (2016). The efficiency of the 4-out-of-5 runs rules scheme for monitoring the ratio of population means of a bivariate normal distribution. *International Journal of Reliability, Quality and Safety Engineering*, 23(05), 1650020.
- Tran, K. P., Castagliola, P., & Celano, G. (2016a). Monitoring the ratio of two normal variables using run rules type control charts. *International Journal of Production Research*, 54(6), 1670-1688.
- Tran, K. P., Castagliola, P., & Celano, G. (2016b). Monitoring the ratio of two normal variables using EWMA type control charts. *Quality and Reliability Engineering International*, 32(5), 1853-1869.
- Tran, K. P., Castagliola, P., & Celano, G. (2016c). The performance of the Shewhart-RZ control chart in the presence of measurement error. *International Journal of Production Research*, 54(24), 7504-7522.
- Tran, K. P., Castagliola, P., & Celano, G. (2018). Monitoring the ratio of population means of a bivariate normal distribution using CUSUM type control charts. *Statistical Papers*, 59(1), 387-413.
- Tran, K. D., Khaliq, Q.U.A., Ahmadi Nadi, A., Nguyen, T. H., & Tran, K. P. (2021). One-sided Shewhart control charts for monitoring the ratio of two normal variables in Short Production Runs. *Journal of Manufacturing Processes*, 69, 273-289.
- Tsay, R. S. (2013). *Multivariate Time Series Analysis: with R and Financial Applications*. John Wiley & Sons.
- Ruey, S. T., & Wood, D. (2018). MTS: All-Purpose Toolkit for Analyzing Multivariate Time Series (MTS) and Estimating Multivariate Volatility Models. R package version 1.0.
- Zhou, L., Zhang, T., Zhang, Z., Lei, Z., & Zhu, S. (2021). A new online quality monitoring method of chain resistance upset butt welding based on Isolation Forest and Local Outlier Factor. *Journal of Manufacturing Processes*, 68, 843-851.

8. Appendices

Appendix A: Derivation of the variance-covariance matrix $\Sigma_{\mathbf{W}}$ in (4).

To calculate $\text{Vec}(\Sigma_{\mathbf{W}})$ in (3), we have,

$$(\mathbf{I}_4 - \Phi \otimes \Phi) = \begin{pmatrix} 1 - \Phi_{XX}^2 & -\Phi_{XX}\Phi_{XY} & -\Phi_{XY}\Phi_{XX} & -\Phi_{XY}^2 \\ -\Phi_{XX}\Phi_{YX} & 1 - \Phi_{XX}\Phi_{YY} & -\Phi_{XY}\Phi_{YX} & -\Phi_{XY}\Phi_{YY} \\ -\Phi_{YX}\Phi_{XX} & -\Phi_{YX}\Phi_{XY} & 1 - \Phi_{YY}\Phi_{XX} & -\Phi_{YY}\Phi_{XY} \\ -\Phi_{YX}^2 & -\Phi_{YX}\Phi_{YY} & -\Phi_{YY}\Phi_{YX} & 1 - \Phi_{YY}^2 \end{pmatrix}$$

After some time-consuming calculations, one can obtain:

$$(\mathbf{I}_4 - \Phi \otimes \Phi)^{-1} = \frac{1}{\Delta} \begin{pmatrix} \Delta_{11} & \Delta_{12} & \Delta_{13} & \Delta_{14} \\ \Delta_{21} & \Delta_{22} & \Delta_{23} & \Delta_{24} \\ \Delta_{31} & \Delta_{32} & \Delta_{33} & \Delta_{34} \\ \Delta_{41} & \Delta_{42} & \Delta_{43} & \Delta_{44} \end{pmatrix}$$

where:

$$\begin{aligned} \Delta &= (\Phi_{XX}\Phi_{YY} - \Phi_{XY}\Phi_{YX} - 1) \\ &\quad \times (\Phi_{XX}^2\Phi_{YY}^2 - 2\Phi_{XX}\Phi_{XY}\Phi_{YX}\Phi_{YY} + \Phi_{XY}^2\Phi_{YX}^2 - \Phi_{XX}^2 - 2\Phi_{XY}\Phi_{YX} - \Phi_{YY}^2 + 1) \end{aligned}$$

and

$$\begin{aligned} \Delta_{11} &= -(\Phi_{XX}\Phi_{YY}^3 - \Phi_{XY}\Phi_{YX}\Phi_{YY}^2 - \Phi_{XX}\Phi_{YY} - \Phi_{XY}\Phi_{YX} - \Phi_{YY}^2 + 1) \\ \Delta_{12} &= \Delta_{13} = \Phi_{XY}(\Phi_{XX}\Phi_{YY}^2 - \Phi_{XY}\Phi_{YX}\Phi_{YY} - \Phi_{XX}) \\ \Delta_{14} &= -\Phi_{XY}^2(\Phi_{XX}\Phi_{YY} - \Phi_{XY}\Phi_{YX} + 1) \\ \Delta_{21} &= \Phi_{YX}(\Phi_{XX}\Phi_{YY}^2 - \Phi_{XY}\Phi_{YX}\Phi_{YY} - \Phi_{XX}) \\ \Delta_{22} &= -(\Phi_{XX}^2\Phi_{YY}^2 - \Phi_{XX}\Phi_{XY}\Phi_{YX}\Phi_{YY} - \Phi_{XX}^2 - \Phi_{XY}\Phi_{YX} - \Phi_{YY}^2 + 1) \\ \Delta_{23} &= -\Phi_{YX}\Phi_{XY}(\Phi_{XX}\Phi_{YY} - \Phi_{XY}\Phi_{YX} + 1) \\ \Delta_{24} &= \Phi_{XY}(\Phi_{XX}^2\Phi_{YY} - \Phi_{XX}\Phi_{XY}\Phi_{YX} - \Phi_{YY}) \\ \Delta_{31} &= \Delta_{21}, \Delta_{32} = \Delta_{23}, \Delta_{33} = \Delta_{22}, \Delta_{34} = \Delta_{24} \\ \Delta_{41} &= -\Phi_{YX}^2(\Phi_{XX}\Phi_{YY} - \Phi_{XY}\Phi_{YX} + 1) \\ \Delta_{42} &= \Phi_{YX}(\Phi_{XX}^2\Phi_{YY} - \Phi_{XX}\Phi_{XY}\Phi_{YX} - \Phi_{YY}) \\ \Delta_{43} &= \Delta_{42} \\ \Delta_{44} &= -(\Phi_{XX}^3\Phi_{YY} - \Phi_{XX}^2\Phi_{XY}\Phi_{YX} - \Phi_{XX}^2 - \Phi_{XX}\Phi_{YY} - \Phi_{XY}\Phi_{YX} + 1) \end{aligned}$$

Accordingly, from these calculations and the formula of $\text{Vec}(\Sigma_{\mathbf{W}})$ in (3), it is resulted that

$$\begin{aligned} \text{Vec}(\Sigma_{\mathbf{W}}) &= \frac{1}{\Delta} \begin{pmatrix} \Delta_{11} & \Delta_{12} & \Delta_{13} & \Delta_{14} \\ \Delta_{21} & \Delta_{22} & \Delta_{23} & \Delta_{24} \\ \Delta_{31} & \Delta_{32} & \Delta_{33} & \Delta_{34} \\ \Delta_{41} & \Delta_{42} & \Delta_{43} & \Delta_{44} \end{pmatrix} \begin{pmatrix} \sigma_{eX}^2 \\ \sigma_{eXY} \\ \sigma_{eXY} \\ \sigma_{eY}^2 \end{pmatrix} \\ &= \frac{1}{\Delta} \begin{pmatrix} \Delta_{11}\sigma_{eX}^2 + (\Delta_{12} + \Delta_{13})\sigma_{eXY} + \Delta_{14}\sigma_{eY}^2 \\ \Delta_{21}\sigma_{eX}^2 + (\Delta_{22} + \Delta_{23})\sigma_{eXY} + \Delta_{24}\sigma_{eY}^2 \\ \Delta_{31}\sigma_{eX}^2 + (\Delta_{32} + \Delta_{33})\sigma_{eXY} + \Delta_{34}\sigma_{eY}^2 \\ \Delta_{41}\sigma_{eX}^2 + (\Delta_{42} + \Delta_{43})\sigma_{eXY} + \Delta_{44}\sigma_{eY}^2 \end{pmatrix} \end{aligned}$$

Finally, this leads us to obtain the variance-covariance matrix $\Sigma_{\mathbf{W}}$ in (4).

Appendix B: Derivation of $\Sigma_{\overline{\mathbf{W}}}$ in eqn. (5)

Let $\mathbf{W}_i = (W_{i,1}, W_{i,2})^\top$ be a stationary bivariate time series with mean vector $\boldsymbol{\mu}_{\mathbf{W}}$ and cross-covariances matrix at lag k as

$$\boldsymbol{\Gamma}(k) = E[(\mathbf{W}_i - \boldsymbol{\mu}_{\mathbf{W}})(\mathbf{W}_{i+k} - \boldsymbol{\mu}_{\mathbf{W}})^\top]_{p \times p} = [\gamma_{j,t}]_{j,t=1,2}.$$

where $\gamma_{jt} = E[(W_{i,j} - \mu_j)(W_{i+k,t} - \mu_t)]$ is the covariance between $W_{i,j}$ and $W_{i+k,t}$ for $k = 0, \pm 1, \pm 2, \pm 3, \dots$. By definition, we have $\Sigma_{\mathbf{W}} = \boldsymbol{\Gamma}(0)$. For the random sample $W_{i,1}, W_{i,2}, \dots, W_{i,n}$, Reinsel (2003) showed that

$$\begin{aligned} \boldsymbol{\mu}_{\overline{\mathbf{W}}} &= \boldsymbol{\mu}_{\mathbf{W}} \\ \Sigma_{\overline{\mathbf{W}}} &= \frac{1}{n^2} \sum_{j=1}^n \sum_{t=1}^n \boldsymbol{\Gamma}(j-t) = \frac{1}{n^2} \sum_{k=-(n-1)}^{n-1} (n-|k|) \boldsymbol{\Gamma}(k). \end{aligned}$$

Adopting this result for VAR(1) autoregressive model, $\Sigma_{\overline{\mathbf{W}}}$ can be obtained as

$$\begin{aligned} \Sigma_{\overline{\mathbf{W}}} &= \frac{1}{n} \Sigma_{\mathbf{W}} + \frac{1}{n^2} \sum_{k=1}^{n-1} (n-k) \boldsymbol{\Gamma}(k) + \frac{1}{n^2} \sum_{k=1}^{n-1} (n-k) \boldsymbol{\Gamma}(-k) \\ &= \frac{1}{n} \Sigma_{\mathbf{W}} + \frac{1}{n^2} \sum_{k=1}^{n-1} (n-k) [\boldsymbol{\Gamma}(k) + \boldsymbol{\Gamma}(k)^\top] \quad (\boldsymbol{\Gamma}(-k) = \boldsymbol{\Gamma}(k)^\top) \\ &= \frac{1}{n} \Sigma_{\mathbf{W}} + \frac{1}{n^2} \sum_{k=1}^{n-1} (n-k) \left[\Sigma_{\mathbf{W}} \boldsymbol{\Phi}^{\top k} + \boldsymbol{\Phi}^k \Sigma_{\mathbf{W}}^\top \right] \quad (\boldsymbol{\Gamma}(k) = \Sigma_{\mathbf{W}} \boldsymbol{\Phi}^{\top k}) \\ &= \frac{1}{n} \Sigma_{\mathbf{W}} + \frac{1}{n} \sum_{k=1}^{n-1} \left[\Sigma_{\mathbf{W}} \boldsymbol{\Phi}^{\top k} + \boldsymbol{\Phi}^k \Sigma_{\mathbf{W}}^\top \right] - \frac{1}{n^2} \sum_{k=1}^{n-1} k \left[\Sigma_{\mathbf{W}} \boldsymbol{\Phi}^{\top k} + \boldsymbol{\Phi}^k \Sigma_{\mathbf{W}}^\top \right]. \quad (23) \end{aligned}$$

In order to further simplify the above relation, we use proposition 1.5.38. of Hubbard and Hubbard (2015) in which they proved that $\sum_{n=0}^{\infty} \boldsymbol{\Phi}^n = (\mathbf{I}_p - \boldsymbol{\Phi})^{-1}$ for a $p \times p$ square matrix $\boldsymbol{\Phi}$ whose absolute values of all its eigenvalues are assumed to be less than 1. Here, we know that this assumption about $\boldsymbol{\Phi}$ is true because it is a necessary and sufficient condition for the stationarity of a VAR(1) autoregressive model. Using the idea of their proof, it can be shown that $\sum_{k=1}^{n-1} \boldsymbol{\Phi}^k = \Lambda(\boldsymbol{\Phi})$ and $\sum_{k=1}^{n-1} k \boldsymbol{\Phi}^k = \Pi(\boldsymbol{\Phi})$, where

$$\begin{aligned} \Lambda(\boldsymbol{\Phi}) &= (\boldsymbol{\Phi} - \boldsymbol{\Phi}^n)(\mathbf{I}_2 - \boldsymbol{\Phi})^{-1} \\ \Pi(\boldsymbol{\Phi}) &= (\boldsymbol{\Phi}^{-1} - \mathbf{I}_2)^{-1} \left((\mathbf{I}_2 - \boldsymbol{\Phi}^{n-1})(\mathbf{I}_2 - \boldsymbol{\Phi})^{-1} - (n-1)\boldsymbol{\Phi}^{n-1} \right) \end{aligned}$$

Rewriting eqn. (23) based on $\Lambda(\boldsymbol{\Phi})$ and $\Pi(\boldsymbol{\Phi})$, after some mathematical calculations we get the expression of $\Sigma_{\overline{\mathbf{W}}}$ in eqn. (5).

Appendix C: Extension to VAR(p) time series observations

The implementation of the Shewhart-type RZ control chart based for VAR(1) time series model is discussed and some interesting theoretical results are also presented in Sections 3 and 4. This Appendix provides some useful outcomes to use the obtained results in Sections 3 and 4 in order to monitor the means ratio Z when the autocorrelation structure between sample observations $(x_1, y_1), \dots, (x_n, y_n)$ follows a VAR model of order p , say VAR(p). The bivariate time series \mathbf{W}_t follows a VAR(p) model with mean vector $\boldsymbol{\mu}_{\mathbf{W}}$ when

$$\mathbf{W}_t - \boldsymbol{\mu}_{\mathbf{W}} = \boldsymbol{\Phi}_1(\mathbf{W}_{t-1} - \boldsymbol{\mu}_{\mathbf{W}}) + \dots + \boldsymbol{\Phi}_p(\mathbf{W}_{t-p} - \boldsymbol{\mu}_{\mathbf{W}}) + \boldsymbol{\varepsilon}_t, \quad (24)$$

where $\boldsymbol{\Phi}_i$ ($i = 1, \dots, p$) are 2×2 coefficients matrices, $\boldsymbol{\Phi}_p \neq 0$, and $\boldsymbol{\varepsilon}_t$ is a bivariate normal vector with mean zero and covariance matrix $\boldsymbol{\Sigma}_{\boldsymbol{\varepsilon}}$. In order to construct the control limits of the RZ chart under the VAR(p) model, in the same way as the VAR(1), the variance-covariance matrix $\boldsymbol{\Sigma}_{\mathbf{W}}$ of \mathbf{W}_t in (24) and then $\boldsymbol{\Sigma}_{\overline{\mathbf{W}}}$ are needed. For the VAR(p) model in (24) we have

$$\boldsymbol{\Sigma}_{\mathbf{W}} = \boldsymbol{\Gamma}(\mathbf{0}) = \boldsymbol{\Phi}_1\boldsymbol{\Gamma}(-1) + \boldsymbol{\Phi}_2\boldsymbol{\Gamma}(-2) + \dots + \boldsymbol{\Phi}_p\boldsymbol{\Gamma}(-p) + \boldsymbol{\Sigma}_{\boldsymbol{\varepsilon}}, \quad (25)$$

where $\boldsymbol{\Gamma}(k)$ is the cross-covariances matrix of \mathbf{W}_t at lag k that can be obtained from the relation

$$\boldsymbol{\Gamma}(k) = \boldsymbol{\Phi}_1\boldsymbol{\Gamma}(k-1) + \boldsymbol{\Phi}_2\boldsymbol{\Gamma}(k-2) + \dots + \boldsymbol{\Phi}_p\boldsymbol{\Gamma}(k-p), \quad \text{for } k > 0, \quad (26)$$

and the fact that $\boldsymbol{\Gamma}(-k) = \boldsymbol{\Gamma}(k)^\top$. From (25), it can be seen that the matrices $\boldsymbol{\Gamma}(-1), \boldsymbol{\Gamma}(-2), \dots, \boldsymbol{\Gamma}(-p)$ are needed to obtain $\boldsymbol{\Sigma}_{\mathbf{W}}$. This makes the problem of finding $\boldsymbol{\Sigma}_{\mathbf{W}}$ and $\boldsymbol{\Sigma}_{\overline{\mathbf{W}}}$ very hard under the VAR(p) model. Here, we are going to tackle this obstacle by using the novel idea of Tsay (2013) to express the VAR(p) model in (24) in a VAR(1) form. Then, one can apply the obtained results for VAR(1) model in Section 4 to monitor the means ratio Z when the autocorrelation structure of within-sample observations is VAR(p). To this end, let us define the $2p$ -dimensional time series \mathbf{Z}_t as

$$\mathbf{Z}_t = \left(\mathbf{W}_t^\top, \mathbf{W}_{t-1}^\top, \dots, \mathbf{W}_{t-p+1}^\top \right)^\top = \begin{pmatrix} W_{1t} \\ W_{2t} \\ W_{1(t-1)} \\ W_{2(t-1)} \\ \vdots \\ W_{1(t-p+1)} \\ W_{2(t-p+1)} \end{pmatrix}_{2p \times 1}. \quad (27)$$

Then, it can be seen that the VAR (p) model in (24) can be represented as a VAR(1) model in terms of \mathbf{Z}_t as

$$\mathbf{Z}_t = \boldsymbol{\Phi}\mathbf{Z}_{t-1} + \mathbf{b}_t, \quad (28)$$

where $\mathbf{b}_t = (\mathbf{a}_t^\top, \mathbf{0}^\top)^\top$ in which $\mathbf{0}$ is a $2(p-1)$ -dimensional zero vector, and

$$\Phi = \begin{pmatrix} \Phi_1 & \Phi_2 & \cdots & \Phi_{p-1} & \Phi_p \\ \mathbf{I}_2 & \mathbf{0}_2 & \cdots & \mathbf{0}_2 & \mathbf{0}_2 \\ \mathbf{0}_2 & \mathbf{I}_2 & \cdots & \mathbf{0}_2 & \mathbf{0}_2 \\ \vdots & \vdots & \ddots & \vdots & \vdots \\ \mathbf{0}_2 & \mathbf{0}_2 & \cdots & \mathbf{I}_2 & \mathbf{0}_2 \end{pmatrix}, \quad (29)$$

where \mathbf{I}_2 and $\mathbf{0}_2$ are the 2×2 identity and zero matrix, respectively. Now, from the definition of time series \mathbf{Z}_t in (27) we have

$$\Sigma_{\mathbf{Z}} = \begin{pmatrix} \Gamma(0) & \Gamma(1) & \cdots & \Gamma(p-1) \\ \Gamma(1)^\top & \Gamma(0) & \cdots & \Gamma(p-2) \\ \vdots & \vdots & \ddots & \vdots \\ \Gamma(p-1)^\top & \Gamma(p-2)^\top & \cdots & \Gamma(0) \end{pmatrix}_{2p \times 2p}. \quad (30)$$

Relation (30) shows that the cross-covariances matrices $\Gamma(k)$ of \mathbf{W}_t for $k = 0, \dots, p-1$, and its variance-covariance matrix $\Sigma_{\mathbf{W}} = \Gamma(0)$, can be obtained once $\Sigma_{\mathbf{Z}}$ is calculated. On the other hand, since \mathbf{Z}_t is a VAR(1) model, from equation (3) we have

$$\text{Vec}(\Sigma_{\mathbf{Z}}) = (\mathbf{I}_{(2p)^2} - \Phi \otimes \Phi)^{-1} \text{Vec}(\Sigma_b), \quad (31)$$

where

$$\Sigma_b = \begin{pmatrix} \Sigma_\varepsilon & \mathbf{0}_2 & \cdots & \mathbf{0}_2 & \mathbf{0}_2 \\ \mathbf{0}_2 & \mathbf{0}_2 & \cdots & \mathbf{0}_2 & \mathbf{0}_2 \\ \mathbf{0}_2 & \mathbf{0}_2 & \cdots & \mathbf{0}_2 & \mathbf{0}_2 \\ \vdots & \vdots & \ddots & \vdots & \vdots \\ \mathbf{0}_2 & \mathbf{0}_2 & \cdots & \mathbf{0}_2 & \mathbf{0}_2 \end{pmatrix}_{2p \times 2p}. \quad (32)$$

Now, the variance-covariance matrix $\Sigma_{\mathbf{W}} = \Gamma(0)$ of the VAR(p) time series \mathbf{W}_t in (24) can be obtained conveniently based on relations (30) and (31). On the other hand, reminding again that \mathbf{Z}_t is a VAR(1) model, the variance-covariance matrix $\Sigma_{\bar{\mathbf{Z}}}$ can be obtained from relations (5) and (31) as

$$\Sigma_{\bar{\mathbf{Z}}} = \begin{pmatrix} \Gamma_{\bar{\mathbf{W}}}(0) & \Gamma_{\bar{\mathbf{W}}}(1) & \cdots & \Gamma_{\bar{\mathbf{W}}}(p-1) \\ \Gamma_{\bar{\mathbf{W}}}(1)^\top & \Gamma_{\bar{\mathbf{W}}}(0) & \cdots & \Gamma_{\bar{\mathbf{W}}}(p-2) \\ \vdots & \vdots & \ddots & \vdots \\ \Gamma_{\bar{\mathbf{W}}}(p-1)^\top & \Gamma_{\bar{\mathbf{W}}}(p-2)^\top & \cdots & \Gamma_{\bar{\mathbf{W}}}(0) \end{pmatrix}_{2p \times 2p}, \quad (33)$$

where $\Gamma_{\bar{\mathbf{W}}}(0) = \Sigma_{\bar{\mathbf{W}}}$. Consequently, given the coefficient matrices Φ_i and the covariance matrix Σ_ε of the VAR(p) model in (24), one can obtain Φ and Σ_b from (29) and (32), calculate matrices $\Sigma_{\mathbf{W}}$ and $\Sigma_{\bar{\mathbf{W}}}$ based on equations (30), (31), and (33), and finally derive the control limits of the RZ chart based on the elements of matrix $\Sigma_{\bar{\mathbf{W}}}$ and relations (7) and (8).

Table 2. Values of LCL (first row) and UCL (second row) for the Shewhart-RZ control chart in the presence of autocorrelation, for $z_0 = 1$, $ARL_0 = 200$, $\Phi_{XX} = \Phi_{YY} = 0.1$, $n \in \{2, 5, 7, 10, 15\}$, $\gamma_X \in \{0.01, 0.2\}$, $\gamma_Y \in \{0.01, 0.2\}$ and $\rho_0 \in \{-0.9, -0.4, 0, 0.4, 0.9\}$.

γ_X	γ_Y	ρ_0	$n = 2$	$n = 5$	$n = 7$	$n = 10$	$n = 15$
0.01	0.01	-0.9	0.9577	0.9711	0.9752	0.9790	0.9827
			1.0442	1.0297	1.0254	1.0214	1.0176
0.01	0.01	-0.4	0.9635	0.9752	0.9787	0.9820	0.9852
			1.0378	1.0255	1.0218	1.0183	1.0151
0.01	0.01	0.0	0.9691	0.9790	0.9820	0.9848	0.9874
			1.0319	1.0215	1.0184	1.0155	1.0127
0.01	0.01	0.4	0.9760	0.9837	0.9860	0.9882	0.9903
			1.0246	1.0166	1.0142	1.0120	1.0098
0.01	0.01	0.9	0.9901	0.9933	0.9943	0.9952	0.9960
			1.0100	1.0067	1.0058	1.0049	1.0040
0.20	0.20	-0.9	0.3940	0.5462	0.5986	0.6502	0.7032
			2.5382	1.8310	1.6707	1.5380	1.4221
0.20	0.20	-0.4	0.4463	0.5938	0.6429	0.6905	0.7388
			2.2405	1.6841	1.5555	1.4482	1.3535
0.20	0.20	0.0	0.5032	0.6428	0.6878	0.7309	0.7741
			1.9875	1.5557	1.4539	1.3682	1.2919
0.20	0.20	0.4	0.5850	0.7093	0.7478	0.7841	0.8199
			1.7094	1.4098	1.3372	1.2753	1.2197
0.20	0.20	0.9	0.8017	0.8687	0.8878	0.9053	0.9220
			1.2474	1.1512	1.1263	1.1046	1.0846
0.01	0.20	-0.9	0.6787	0.7585	0.7861	0.8134	0.8416
			1.8340	1.4489	1.3619	1.2901	1.2274
0.01	0.20	-0.4	0.6860	0.7640	0.7910	0.8177	0.8452
			1.8144	1.4385	1.3535	1.2833	1.2221
0.01	0.20	0.0	0.6920	0.7686	0.7951	0.8213	0.8482
			1.7986	1.4299	1.3466	1.2778	1.2177
0.01	0.20	0.4	0.6983	0.7732	0.7992	0.8249	0.8513
			1.7825	1.4213	1.3397	1.2722	1.2134
0.01	0.20	0.9	0.7063	0.7793	0.8045	0.8295	0.8552
			1.7622	1.4103	1.3308	1.2651	1.2078
0.20	0.01	-0.9	0.5452	0.6902	0.7342	0.7751	0.8148
			1.4735	1.3184	1.2720	1.2293	1.1883
0.20	0.01	-0.4	0.5511	0.6952	0.7388	0.7792	0.8183
			1.4577	1.3089	1.2641	1.2229	1.1831
0.20	0.01	0.0	0.5560	0.6993	0.7426	0.7826	0.8212
			1.4450	1.3011	1.2577	1.2176	1.1790
0.20	0.01	0.4	0.5610	0.7036	0.7465	0.7860	0.8242
			1.4321	1.2932	1.2512	1.2123	1.1747
0.20	0.01	0.9	0.5675	0.7091	0.7514	0.7905	0.8280
			1.4158	1.2833	1.2429	1.2055	1.1693

Table 3. The $(ARL_1, SDRRL_1)$ values of the Shewhart-RZ control chart in the presence of autocorrelation for $\Phi_{XX} = \Phi_{YY} = 0.1$ (first row), $\Phi_{XX} = \Phi_{YY} = 0.7$ (second row), $\gamma_X = \gamma_Y \in \{0.01, 0.2\}$, $\rho_0 \in \{-0.9, -0.4, 0, 0.4, 0.9\}$, $\rho_1 \in \{2, 5, 7, 10, 15\}$ and $ARL_0 = 200$.

τ	$(\gamma_X = 0.01, \gamma_Y = 0.01)$					$(\gamma_X = 0.2, \gamma_Y = 0.2)$					
	$n = 2$	$n = 5$	$n = 7$	$n = 10$	$n = 15$	$n = 2$	$n = 5$	$n = 7$	$n = 10$	$n = 15$	
0.90	(1.0,0.0)	(1.0,0.0)	(1.0,0.0)	(1.0,0.0)	(1.0, 0.0)	$\rho_0 = -0.9$	(140.1,139.6)	(86.5,86.0)	(67.4, 66.9)	(49.4,48.9)	(32.9,32.4)
	(1.1,0.3)	(1.0,0.1)	(1.0,0.1)	(1.0,0.0)	(1.0,0.0)	(189.7,189.2)	(179.0,178.5)	(171.9,171.4)	(161.4,160.9)	(145.2,144.7)	
	(57.4,56.9)	(24.8,24.3)	(16.9,16.4)	(10.8,10.3)	(6.3,5.8)	(199.3,198.8)	(197.9,197.4)	(197.0,196.5)	(195.6,195.1)	(193.4,192.9)	
	(115.1,114.6)	(97.9,97.4)	(88.5,88.0)	(76.7,76.2)	(61.6,61.1)	(199.9,199.4)	(199.8,199.3)	(199.7,199.2)	(199.6,199.1)	(199.3,198.8)	
	(58.3,57.8)	(25.4,24.9)	(17.3,16.8)	(11.1,10.6)	(6.5,5.9)	(199.3,198.8)	(197.9,197.4)	(197.0,196.5)	(195.7,195.2)	(193.5,193.0)	
1.01	(116.1,115.6)	(99.0,98.5)	(89.6,89.1)	(77.8,77.3)	(62.6,62.1)	(199.9,199.4)	(199.8,199.3)	(199.7,199.2)	(199.6,199.1)	(199.4,198.9)	
	(1.0,0.0)	(1.0,0.0)	(1.0,0.0)	(1.0,0.0)	(1.0,0.0)	(148.5,148.0)	(97.4,96.9)	(77.9,77.4)	(58.7,58.2)	(40.3,39.8)	
	(1.2,0.5)	(1.1,0.2)	(1.0,0.1)	(1.0,0.1)	(1.0,0.0)	(191.5,191.0)	(182.5,182.0)	(176.5,176.0)	(167.4,166.9)	(153.1,152.6)	
	(1.0,0.0)	(1.0,0.0)	(1.0,0.0)	(1.0,0.0)	(1.0, 0.0)	$\rho_0 = -0.4$	(127.6,127.1)	(70.9,70.4)	(53.0,52.5)	(37.2,36.7)	(23.6,23.1)
	(1.0,0.1)	(1.0,0.0)	(1.0,0.0)	(1.0,0.0)	(1.0,0.0)	(187.8,187.3)	(174.5,174.0)	(165.6,165.1)	(152.7,152.2)	(133.5,133.0)	
0.99	(43.8,43.3)	(17.3,16.8)	(11.4,10.9)	(7.1,6.6)	(4.1,3.6)	(199.0,198.5)	(197.2,196.7)	(196.0,195.5)	(194.1,193.6)	(191.2,190.7)	
	(98.9,98.4)	(81.4,80.9)	(72.3,71.8)	(61.1,60.6)	(47.5,47.0)	(199.9,199.4)	(199.7,199.2)	(199.6,199.1)	(199.5,199.0)	(199.1,198.6)	
	(44.6,44.1)	(17.7,17.2)	(11.7,11.2)	(7.3,6.8)	(4.2,3.7)	(199.1,198.6)	(197.2,196.7)	(196.0,195.5)	(194.3,193.8)	(191.3,190.8)	
	(99.9,99.4)	(82.5,82.0)	(73.3,72.8)	(62.1,61.6)	(48.3,47.8)	(199.9,199.4)	(199.7,199.2)	(199.6,199.1)	(199.5,199.0)	(199.2,198.7)	
	(1.0,0.0)	(1.0,0.0)	(1.0,0.0)	(1.0,0.0)	(1.0,0.0)	(137.1,136.6)	(81.6, 81.1)	(62.6,62.1)	(45.2,44.7)	(29.5,29.0)	
1.10	(1.1,0.2)	(1.0,0.1)	(1.0,0.0)	(1.0,0.0)	(1.0,0.0)	(189.9,189.4)	(178.7,178.2)	(171.1,170.6)	(159.8,159.3)	(142.5,142.0)	
	(1.0,0.0)	(1.0,0.0)	(1.0,0.0)	(1.0,0.0)	(1.0,0.0)	$\rho_0 = 0.0$	(111.9,111.4)	(54.7,54.2)	(38.9,38.4)	(26.0,25.5)	(15.7,15.2)
	(1.0,0.0)	(1.0,0.0)	(1.0,0.0)	(1.0,0.0)	(1.0,0.0)	(184.9,184.4)	(167.9,167.4)	(156.7,156.2)	(141.0,140.5)	(118.5,118.0)	
	(31.3,30.8)	(11.2,10.7)	(7.3,6.7)	(4.5,4.0)	(2.7,2.1)	(198.7,198.2)	(196.1,195.6)	(194.4,193.9)	(191.9,191.4)	(187.9,187.4)	
	(80.7,80.2)	(64.0,63.5)	(55.6,55.1)	(45.8,45.3)	(34.3, 33.8)	(199.9,199.4)	(199.7,199.2)	(199.5,199.0)	(199.3,198.8)	(198.9,198.4)	
1.01	(32.0,31.5)	(11.5,11.0)	(7.5,6.9)	(4.6,4.1)	(2.7,2.2)	(198.7,198.2)	(196.2,195.7)	(194.6,194.1)	(192.1,191.6)	(188.1,187.6)	
	(81.8,81.3)	(65.0,64.5)	(56.6,56.1)	(46.6,46.1)	(35.0, 34.5)	(199.9,199.4)	(199.7,199.2)	(199.5,199.0)	(199.3,198.8)	(198.9,198.4)	
	(1.0,0.0)	(1.0,0.0)	(1.0,0.0)	(1.0,0.0)	(1.0, 0.0)	(122.4,121.9)	(64.5,64.0)	(47.2,46.7)	(32.5,32.0)	(20.1,19.6)	
	(1.0,0.1)	(1.0,0.0)	(1.0,0.0)	(1.0,0.0)	(1.0,0.0)	(187.5,187.0)	(173.1,172.6)	(163.4,162.9)	(149.3,148.8)	(128.6,128.1)	
	(1.0,0.0)	(1.0,0.0)	(1.0,0.0)	(1.0,0.0)	(1.0,0.0)	$\rho_0 = 0.4$	(85.4, 84.9)	(33.8,33.3)	(22.4,21.9)	(14.0,13.5)	(8.0,7.5)
0.90	(1.0,0.0)	(1.0,0.0)	(1.0,0.0)	(1.0,0.0)	(1.0,0.0)	(178.5,178.0)	(154.0,153.5)	(138.8,138.3)	(118.6,118.1)	(92.5,92.0)	
	(17.4,16.9)	(5.6,5.1)	(3.6,3.1)	(2.3,1.7)	(1.5,0.9)	(197.9,197.4)	(193.7,193.2)	(191.0,190.5)	(187.0,186.5)	(180.6,180.1)	
	(54.9,54.4)	(41.0,40.5)	(34.5,34.0)	(27.2,26.7)	(19.3,18.8)	(199.8,199.3)	(199.5,199.0)	(199.3,198.8)	(198.9,198.4)	(198.2,197.7)	
	(17.8,17.3)	(5.8,5.2)	(3.7,3.2)	(2.4,1.8)	(1.5,0.9)	(197.9,197.4)	(193.8,193.3)	(191.2,190.7)	(187.2,186.7)	(181.0,180.5)	
	(55.9,55.4)	(41.8,41.3)	(35.2,34.7)	(27.9,27.4)	(19.8, 19.3)	(199.8,199.3)	(199.5,199.0)	(199.3,198.8)	(198.9,198.4)	(198.2,197.7)	
1.10	(1.0,0.0)	(1.0,0.0)	(1.0,0.0)	(1.0,0.0)	(1.0, 0.0)	(96.6,96.1)	(41.5,41.0)	(28.3,27.8)	(18.1,17.6)	(10.5,10.0)	
	(1.0,0.0)	(1.0,0.0)	(1.0,0.0)	(1.0,0.0)	(1.0,0.0)	(182.1,181.6)	(161.0,160.5)	(147.4,146.9)	(128.8,128.3)	(103.7,103.2)	
	(1.0,0.0)	(1.0,0.0)	(1.0,0.0)	(1.0,0.0)	(1.0,0.0)	$\rho_0 = 0.9$	(14.1,13.6)	(3.2,2.7)	(2.1,1.5)	(1.4,0.8)	(1.1,0.3)
	(1.0,0.0)	(1.0,0.0)	(1.0,0.0)	(1.0,0.0)	(1.0,0.0)	(188.7,188.2)	(167.5,167.0)	(155.4,154.9)	(140.0,139.5)	(119.5,119.0)	
	(1.7,1.1)	(1.0,0.2)	(1.0,0.1)	(1.0,0.0)	(1.0,0.0)	(199.0,198.5)	(197.3,196.8)	(196.0,195.5)	(193.8,193.3)	(189.9,189.4)	
0.99	(7.0,6.5)	(4.5,4.0)	(3.6,3.0)	(2.7,2.1)	(1.9,1.3)	(188.7,188.2)	(168.0,167.5)	(156.2,155.6)	(140.9,140.4)	(120.5,120.0)	
	(1.8,1.1)	(1.0,0.2)	(1.0,0.1)	(1.0,0.0)	(1.0,0.0)	(199.0,198.5)	(197.3,196.8)	(196.1,195.6)	(193.9,193.4)	(190.1,189.6)	
	(7.2,6.7)	(4.6,4.1)	(3.7,3.1)	(2.7,2.2)	(1.9,1.3)	(18.5,18.0)	(4.3,3.7)	(2.6,2.1)	(1.7,1.1)	(1.2 0.5)	
	(1.0,0.0)	(1.0,0.0)	(1.0,0.0)	(1.0,0.0)	(1.0,0.0)	(129.6,129.1)	(77.3,76.8)	(56.7,56.2)	(37.6,37.1)	(21.7,21.2)	
	(1.0,0.0)	(1.0,0.0)	(1.0,0.0)	(1.0,0.0)	(1.0,0.0)						

Table 4. The $(ARL_1, SDRRL_1)$ values of the Shewhart-RZ control chart in the presence of autocorrelation for $\Phi_{XX} = \Phi_{YY} = 0.1$ (first row), $\Phi_{XX} = \Phi_{YY} = 0.7$ (second row), $\gamma_X \in \{0.01, 0.2\}$, $\gamma_Y \in \{0.01, 0.2\}$, $\gamma_X \neq \gamma_Y$, $\rho_0 = \rho_1$, $n \in \{2, 5, 7, 10, 15\}$ and $ARL_0 = 200$.

τ	$(\gamma_X = 0.01, \gamma_Y = 0.2)$					$(\gamma_X = 0.2, \gamma_Y = 0.01)$				
	$n = 2$	$n = 5$	$n = 7$	$n = 10$	$n = 15$	$n = 2$	$n = 5$	$n = 7$	$n = 10$	$n = 15$
	$\rho_0 = \rho_1 = -0.9$									
0.90	(34.6,34.1)	(16.9,16.4)	(12.1,11.6)	(8.3,7.7)	(5.2,4.6)	(116.3,115.8)	(44.6,44.1)	(28.7,28.2)	(17.2,16.7)	(9.2,8.7)
	(61.5,61.0)	(54.0,53.5)	(49.7,49.2)	(44.2,43.7)	(36.7,36.2)	(262.2,261.7)	(216.4,215.9)	(192.3,191.8)	(162.6,162.1)	(126.1,125.6)
0.99	(181.6,181.1)	(177.4,176.9)	(174.7,174.2)	(170.8,170.3)	(164.7,164.2)	(212.9,212.4)	(207.8,207.2)	(204.4,203.9)	(199.7,199.2)	(192.1,191.6)
	(183.7,183.2)	(183.0,182.5)	(182.6,182.1)	(181.8,181.3)	(181.8,181.3)	(215.5,215.0)	(215.0,214.5)	(214.7,214.2)	(214.1,213.6)	(213.2,212.7)
1.01	(212.8,212.3)	(207.8,207.3)	(204.5,204.0)	(199.8,199.3)	(192.4,191.9)	(181.8,181.3)	(177.7,177.2)	(175.1,174.6)	(171.2,170.7)	(165.2,164.7)
	(215.4,214.9)	(214.9,214.4)	(214.5,214.0)	(214.0,213.5)	(213.1,212.6)	(183.9,183.4)	(183.5,183.0)	(183.2,182.7)	(182.8,182.3)	(182.0,181.5)
1.10	(129.7,129.2)	(54.0,53.5)	(35.9,35.4)	(22.2,21.7)	(12.2,11.7)	(41.6,41.1)	(21.3,20.8)	(15.5,15.0)	(10.7,10.2)	(6.7,6.2)
	(265.9,265.4)	(225.1,224.6)	(203.0,202.5)	(175.1,174.6)	(139.5,139.0)	(69.7,69.2)	(62.1,61.6)	(57.7,57.2)	(51.9,51.4)	(43.9,43.4)
	$\rho_0 = \rho_1 = -0.4$									
0.90	(32.6,32.1)	(15.8,15.3)	(11.3,10.8)	(7.7,7.2)	(4.8,4.3)	(114.4,113.9)	(43.0,42.5)	(27.5,27.0)	(16.3, 15.8)	(8.7,8.2)
	(58.5,58.0)	(51.2,50.7)	(47.1,46.6)	(41.7,41.2)	(34.6, 34.1)	(263.3,262.8)	(216.1,215.6)	(191.5,191.0)	(161.3,160.8)	(124.3,123.8)
0.99	(180.7,180.2)	(176.4,175.9)	(173.6,173.1)	(169.6,169.1)	(163.2,162.7)	(213.5,213.0)	(208.1,207.6)	(204.6,204.1)	(199.6,199.1)	(191.7,191.2)
	(183.0,182.5)	(182.5,182.0)	(182.2,181.7)	(181.8,181.3)	(181.0,180.5)	(216.2,215.7)	(215.7,215.2)	(215.4,214.9)	(214.8,214.3)	(213.8,213.3)
1.01	(213.4,212.9)	(208.1,207.6)	(204.7,204.2)	(199.8,199.3)	(192.0,191.5)	(181.0,180.5)	(176.7,176.2)	(174.0,173.5)	(170.0,169.5)	(163.7,163.2)
	(216.1,215.6)	(215.6,215.1)	(215.2,214.7)	(214.7,214.2)	(213.7,213.2)	(183.1,182.6)	(182.7,182.2)	(182.4,181.9)	(182.0,181.5)	(181.2,180.7)
1.10	(127.9,127.4)	(52.3,51.8)	(34.4,33.9)	(21.1,20.6)	(11.5,11.0)	(39.3,38.8)	(20.0,19.5)	(14.5,14.0)	(10.0,9.5)	(6.3,5.8)
	(267.4,266.9)	(225.3,224.8)	(202.6,202.1)	(174.0,173.5)	(137.8,137.3)	(66.5,66.0)	(59.1,58.6)	(54.8,54.3)	(49.2,48.7)	(41.5,41.0)
	$\rho_0 = \rho_1 = 0.0$									
0.90	(31.0,30.5)	(15.0,14.5)	(10.7,10.2)	(7.3,6.8)	(4.6,4.0)	(112.8,112.3)	(41.7,41.2)	(26.5,26.0)	(15.6,15.1)	(8.3,7.8)
	(55.9,55.4)	(48.8,48.3)	(44.9,44.4)	(39.7,39.2)	(32.9,32.4)	(264.2,263.7)	(215.9,215.4)	(190.8,190.3)	(160.1,159.6)	(122.8,122.3)
0.99	(180.0,179.5)	(175.5,175.0)	(172.6,172.1)	(168.5,168.0)	(161.9,161.4)	(214.0,213.5)	(208.4,207.9)	(204.8,204.3)	(199.6,199.1)	(191.4,190.9)
	(182.3,181.8)	(181.9,181.4)	(181.6,181.1)	(181.1,180.6)	(180.3,179.8)	(216.9,216.4)	(216.4,215.9)	(216.0,215.5)	(215.4,214.9)	(214.4,213.9)
1.01	(213.9,213.4)	(208.4,207.9)	(204.9,204.4)	(199.8,199.3)	(191.7,191.2)	(180.2,179.7)	(175.8,175.3)	(173.0,172.5)	(168.9,168.4)	(162.4,161.9)
	(216.7,216.2)	(216.2,215.7)	(215.8,215.3)	(215.3,214.8)	(214.3,213.8)	(182.5,182.0)	(182.1,181.6)	(181.8,181.3)	(181.3,180.8)	(180.5,180.0)
1.10	(126.4,125.9)	(50.8,50.3)	(33.3,32.8)	(20.3,19.7)	(11.0,10.5)	(37.4,36.9)	(18.9,18.4)	(13.7,13.2)	(9.4,8.9)	(5.9,5.4)
	(268.7,268.2)	(225.4,224.9)	(202.1,201.6)	(173.0,172.5)	(136.4,135.9)	(63.9,63.4)	(56.6,56.1)	(52.5,52.0)	(47.0,46.5)	(39.6,39.1)
	$\rho_0 = \rho_1 = 0.4$									
0.90	(29.3,28.8)	(14.1,13.6)	(10.1,9.6)	(6.8,6.3)	(4.3,3.8)	(111.2,110.7)	(40.4,39.9)	(25.5,25.0)	(14.9,14.4)	(7.9,7.3)
	(53.3,52.8)	(46.5,46.0)	(42.7,42.2)	(37.7,37.2)	(31.2,30.7)	(265.1,264.6)	(215.7,215.2)	(190.1,189.6)	(158.9,158.4)	(121.2,120.7)
0.99	(179.2,178.7)	(174.6,174.1)	(171.6,171.1)	(167.3,166.8)	(160.6,160.1)	(214.6,214.1)	(208.7,208.2)	(205.0,204.5)	(199.6,199.1)	(191.1,190.6)
	(181.6,181.1)	(181.1,180.6)	(180.8,180.3)	(180.3,179.8)	(179.5,179.0)	(217.6,217.1)	(217.0,216.5)	(216.6,216.1)	(216.0,215.5)	(215.0,214.5)
1.01	(214.5,214.0)	(208.8,208.3)	(205.1,204.6)	(199.7,199.2)	(191.4,190.9)	(179.4,178.9)	(174.9,174.4)	(172.0,171.5)	(167.7,167.2)	(161.1,160.6)
	(217.4,216.9)	(216.9,216.4)	(216.5,216.0)	(215.9,215.4)	(214.9,214.4)	(181.8,181.3)	(181.3,180.8)	(181.0,180.5)	(180.5,180.0)	(179.7,179.2)
1.10	(124.8,124.3)	(49.4,48.8)	(32.1,31.6)	(19.4, 18.9)	(10.4,9.9)	(35.6,35.1)	(17.9, 17.4)	(13.0,12.4)	(8.9,8.4)	(5.6,5.1)
	(269.9,269.4)	(225.4,224.9)	(201.7,201.2)	(172.0,171.5)	(134.9,134.4)	(61.1, 60.6)	(54.1,53.6)	(50.1,49.6)	(44.8,44.3)	(37.6,37.1)
	$\rho_0 = \rho_1 = 0.9$									
0.90	(27.3,26.8)	(13.1,12.5)	(9.3,8.8)	(6.3,5.8)	(4.0,3.5)	(109.1,108.6)	(38.7,38.2)	(24.2,23.7)	(14.1,13.5)	(7.3,6.8)
	(49.9,49.4)	(43.4,42.9)	(39.8,39.3)	(35.2,34.7)	(29.0,28.5)	(266.3,265.8)	(215.3,214.8)	(189.0,188.5)	(157.3,156.8)	(119.1,118.6)
0.99	(178.1,177.6)	(173.3,172.8)	(170.2,169.7)	(165.7,165.2)	(158.7,158.2)	(215.4,214.9)	(209.2,208.7)	(205.2,204.7)	(199.5,199.0)	(190.6,190.1)
	(180.6,180.1)	(180.1,179.6)	(179.8,179.3)	(179.3,178.8)	(178.4,177.9)	(218.6,218.1)	(218.0,217.5)	(217.6,217.1)	(216.9,216.4)	(215.8,215.3)
1.01	(215.3,214.8)	(209.2,208.7)	(205.3,204.8)	(199.7,199.2)	(191.0,190.5)	(178.4,177.9)	(173.6,173.1)	(170.6,170.1)	(166.2,165.7)	(159.3,158.8)
	(218.4,217.9)	(217.8,217.3)	(217.4,216.9)	(216.8,216.3)	(215.7,215.2)	(180.8,180.3)	(180.3,179.8)	(180.0,179.5)	(179.5,179.0)	(178.7,178.2)
1.10	(122.7,122.2)	(47.5,47.0)	(30.6,30.1)	(18.3,17.8)	(9.8,9.3)	(33.2,32.7)	(16.6,16.1)	(12.0,11.5)	(8.2,7.7)	(5.2,4.6)
	(271.5,271.0)	(225.4,224.9)	(201.0,200.5)	(170.6,170.1)	(132.9,132.4)	(57.5,57.0)	(50.8,50.3)	(47.0,46.5)	(41.9,41.4)	(35.1,34.6)

Table 5. The $(ARL_1, SDRLL_1)$ values of the Shewhart-RZ control chart in the presence of autocorrelation for $\Phi_{XX} = 0.1, \Phi_{YY} = 0.7$ (first row), $\Phi_{XX} = 0.7, \Phi_{YY} = 0.1$ (second row), $\gamma_X \in \{0.01, 0.2\}, \gamma_Y \in \{0.01, 0.2\}, \gamma_X = \gamma_Y, \rho_0 = \rho_1, n \in \{2, 5, 7, 10, 15\}$ and $ARL_0 = 200$.

τ	$(\gamma_X = 0.01, \gamma_Y = 0.01)$					$(\gamma_X = 0.2, \gamma_Y = 0.2)$				
	$n = 2$	$n = 5$	$n = 7$	$n = 10$	$n = 15$	$n = 2$	$n = 5$	$n = 7$	$n = 10$	$n = 15$
0.90	(1.0,0.1)	(1.0,0.0)	(1.0,0.0)	(1.0,0.0)	$\rho_0 = \rho_1 = -0.9$ (1.0,0.0)	(130.7,130.2)	(101.3,100.8)	(91.1,90.6)	(80.0,79.5)	(66.8,66.3)
	(1.0,0.1)	(1.0,0.0)	(1.0,0.0)	(1.0,0.0)	(1.0,0.0)	(221.7,221.2)	(205.7,205.2)	(190.8,190.3)	(169.3,168.8)	(139.6,139.1)
	(82.6,82.1)	(59.2,58.7)	(50.0,49.5)	(40.0,39.5)	(29.1,28.6)	(194.5,194.0)	(192.1,191.6)	(191.4,190.9)	(190.7,190.2)	(189.9,189.4)
	(86.2,85.7)	(62.5,62.0)	(52.8,52.3)	(42.2,41.7)	(30.6, 30.1)	(205.0,204.5)	(206.8,206.3)	(207.1,206.6)	(207.2,206.7)	(206.9,206.4)
	(87.3,86.8)	(63.5,63.0)	(53.7,53.2)	(43.0,42.5)	(31.3, 30.8)	(204.9,204.4)	(206.7,206.2)	(207.1,206.6)	(207.1,206.6)	(206.9,206.4)
1.01	(83.7,83.2)	(60.2,59.7)	(50.8,50.3)	(40.8,40.3)	(29.7,29.2)	(194.6,194.1)	(192.2,191.7)	(191.5,191.0)	(190.8,190.3)	(190.0,189.5)
	(1.0,0.1)	(1.0,0.0)	(1.0,0.0)	(1.0,0.0)	(1.0,0.0)	(222.6,222.1)	(210.7,210.2)	(197.9,197.4)	(178.8,178.3)	(151.2,150.7)
	(1.0,0.1)	(1.0,0.0)	(1.0,0.0)	(1.0,0.0)	(1.0,0.0)	(137.6,137.1)	(110.0,109.5)	(100.3,99.8)	(89.5,89.0)	(76.2,75.7)
	(1.0,0.0)	(1.0,0.0)	(1.0,0.0)	(1.0,0.0)	$\rho_0 = \rho_1 = -0.4$ (1.0,0.0)	(119.8,119.3)	(88.0, 87.5)	(77.7,77.2)	(66.9,66.4)	(54.6,54.1)
	(1.0,0.0)	(1.0,0.0)	(1.0,0.0)	(1.0,0.0)	(1.0,0.0)	(224.8,224.3)	(205.5,205.0)	(188.1,187.6)	(163.8,163.3)	(131.4,130.9)
0.99	(70.1,69.6)	(48.7,48.2)	(40.5,40.0)	(31.9,31.4)	(22.7,22.2)	(193.5,193.0)	(190.4,189.9)	(189.5,189.0)	(188.6,188.1)	(187.6,187.1)
	(73.8,73.3)	(52.0,51.5)	(43.3,42.8)	(34.0,33.5)	(24.1,23.6)	(205.9,205.4)	(208.3,207.8)	(208.7,208.2)	(208.8,208.3)	(208.5,208.0)
	(74.9,74.4)	(52.9,52.4)	(44.1,43.6)	(34.7,34.2)	(24.6,24.1)	(205.9,205.4)	(208.2,207.7)	(208.6,208.1)	(208.7,208.2)	(208.4,207.9)
	(71.1,70.6)	(49.6,49.1)	(41.3,40.8)	(32.6,32.0)	(23.2,22.7)	(193.5,193.0)	(190.5,190.0)	(189.6,189.1)	(188.8,188.3)	(187.8,187.3)
	(1.0,0.0)	(1.0,0.0)	(1.0,0.0)	(1.0,0.0)	(1.0,0.0)	(226.1,225.6)	(211.6,211.1)	(196.5,196.0)	(174.5,174.0)	(143.8,143.3)
1.10	(1.0,0.0)	(1.0,0.0)	(1.0,0.0)	(1.0,0.0)	(1.0,0.0)	(127.5,127.0)	(97.0,96.5)	(86.9,86.4)	(76.1,75.6)	(63.4,62.9)
	(1.0,0.0)	(1.0,0.0)	(1.0,0.0)	(1.0,0.0)	$\rho_0 = \rho_1 = 0.0$ (1.0,0.0)	(106.9,106.4)	(73.9,73.4)	(64.0,63.5)	(54.2,53.7)	(43.3,42.8)
	(1.0,0.0)	(1.0,0.0)	(1.0,0.0)	(1.0,0.0)	(1.0,0.0)	(228.6,228.1)	(204.8,204.3)	(184.7,184.2)	(157.6,157.1)	(122.7,122.2)
	(58.0,57.5)	(39.3,38.8)	(32.3,31.8)	(25.0,24.5)	(17.4,16.9)	(192.1,191.6)	(188.3,187.8)	(187.1,186.6)	(186.1,185.6)	(184.8,184.3)
	(61.8,61.3)	(42.4,41.9)	(34.9,34.4)	(26.9,26.4)	(18.7,18.2)	(207.2,206.7)	(210.2,209.7)	(210.7,210.2)	(210.9,210.4)	(210.5,210.0)
1.01	(62.8,62.3)	(43.2,42.7)	(35.6,35.1)	(27.5,27.0)	(19.1,18.6)	(207.2,206.7)	(210.1,209.6)	(210.6,210.1)	(210.8,210.3)	(210.4,209.9)
	(59.0,58.5)	(40.1,39.6)	(33.0,32.5)	(25.6,25.0)	(17.9,17.4)	(192.1,191.6)	(188.4,187.9)	(187.3,186.8)	(186.2,185.7)	(185.0,184.5)
	(1.0,0.0)	(1.0,0.0)	(1.0,0.0)	(1.0,0.0)	(1.0,0.0)	(230.4,229.9)	(212.2,211.7)	(194.4,193.9)	(169.4,168.9)	(135.8,135.3)
	(1.0,0.0)	(1.0,0.0)	(1.0,0.0)	(1.0,0.0)	(1.0,0.0)	(115.2,114.7)	(82.9,82.4)	(73.0,72.5)	(62.8,62.3)	(51.2,50.7)
	(1.0,0.0)	(1.0,0.0)	(1.0,0.0)	(1.0,0.0)	$\rho_0 = \rho_1 = 0.4$ (1.0,0.0)	(87.2,86.7)	(55.5, 55.0)	(47.1,46.6)	(39.1,38.6)	(30.6,30.1)
0.99	(1.0, 0.0)	(1.0, 0.0)	(1.0,0.0)	(1.0,0.0)	(1.0, 0.0)	(234.2,233.7)	(202.9,202.4)	(179.1,178.6)	(148.7,148.2)	(111.4,110.9)
	(43.8,43.3)	(28.9,28.4)	(23.4,22.9)	(17.8, 17.3)	(12.2,11.7)	(189.5,189.0)	(184.6,184.1)	(183.1,182.6)	(181.7,181.2)	(180.1,179.6)
	(47.4,46.9)	(31.8,31.3)	(25.7,25.2)	(19.5,19.0)	(13.2, 12.7)	(209.6,209.1)	(213.5,213.0)	(214.2,213.7)	(214.3,213.8)	(213.8,213.3)
	(48.3,47.8)	(32.5,31.9)	(26.3,25.8)	(20.0,19.5)	(13.5, 13.0)	(209.5,209.0)	(213.4,212.9)	(214.0,213.5)	(214.2,213.7)	(213.7,213.2)
	(44.6, 44.1)	(29.5,29.0)	(24.0,23.5)	(18.3,17.8)	(12.5,12.0)	(189.6,189.1)	(184.7,184.2)	(183.3,182.8)	(181.9,181.4)	(180.4,179.9)
1.10	(1.0,0.0)	(1.0,0.0)	(1.0,0.0)	(1.0,0.0)	(1.0, 0.0)	(237.1,236.6)	(212.2,211.7)	(190.7,190.2)	(161.8,161.3)	(125.0,124.5)
	(1.0,0.0)	(1.0,0.0)	(1.0,0.0)	(1.0,0.0)	(1.0,0.0)	(96.1,95.6)	(63.9,63.4)	(55.1,54.6)	(46.5,46.0)	(37.1,36.6)
	(1.0,0.0)	(1.0,0.0)	(1.0,0.0)	(1.0,0.0)	$\rho_0 = \rho_1 = 0.9$ (1.0,0.0)	(45.1,44.6)	(26.1,25.6)	(22.0,21.5)	(18.1,17.6)	(14.1,13.6)
	(22.4,21.9)	(14.9,14.4)	(12.0,11.5)	(9.0,8.4)	(6.0,5.5)	(244.8,244.3)	(194.7,194.2)	(165.4,164.9)	(130.6,130.1)	(91.3,90.8)
	(25.4,24.8)	(17.1,16.5)	(13.6,13.1)	(10.1,9.6)	(6.7, 6.1)	(180.8,180.3)	(173.3,172.8)	(171.3,170.8)	(169.4,168.9)	(167.3,166.8)
1.01	(25.9,25.4)	(17.5,17.0)	(14.0,13.5)	(10.4,9.8)	(6.8,6.3)	(217.8,217.3)	(223.8,223.3)	(224.6,224.1)	(224.5,224.0)	(223.3,222.8)
	(22.9,22.4)	(15.3,14.8)	(12.3,11.8)	(9.2,8.7)	(6.2,5.7)	(217.6,217.1)	(223.6,223.1)	(224.4,223.9)	(224.3,223.8)	(223.1,222.6)
	(1.0,0.0)	(1.0,0.0)	(1.0,0.0)	(1.0,0.0)	(1.0,0.0)	(181.0,180.5)	(173.6,173.1)	(171.6,171.1)	(169.8,169.3)	(167.6,167.1)
	(1.0,0.0)	(1.0,0.0)	(1.0,0.0)	(1.0,0.0)	(1.0,0.0)	(251.7,251.2)	(207.8,207.3)	(179.6,179.1)	(145.3,144.8)	(105.0,104.5)
	(1.0,0.0)	(1.0,0.0)	(1.0,0.0)	(1.0,0.0)	(1.0,0.0)	(52.9,52.4)	(31.7,31.2)	(26.9,26.4)	(22.4,21.9)	(17.7,17.2)

Table 6. The $(ARL_1, SDRRL_1)$ values of the Shewhart-RZ control chart in the presence of autocorrelation for $\Phi_{XX} = 0.1, \Phi_{YY} = 0.7$ (first row), $\Phi_{XX} = 0.7, \Phi_{YY} = 0.1$ (second row), $\gamma_X \in \{0.01, 0.2\}, \gamma_Y \in \{-0.9, -0.4, 0.0, 0.4, 0.9\}, \rho_0 = \rho_1, n \in \{2, 5, 7, 10, 15\}$ and $ARL_0 = 200$.

τ	$(\gamma_X = 0.01, \gamma_Y = 0.2)$									
	$n = 2$	$n = 5$	$n = 7$	$n = 10$	$n = 15$	$n = 15$				
	$(\gamma_X = 0.2, \gamma_Y = 0.01)$									
	$\rho_0 = \rho_1 = -0.9$									
0.90	(58.3,57.7)	(50.6,50.1)	(46.4,45.9)	(41.1,40.6)	(34.1,33.6)	(17.4,116.9)	(47.3,46.8)	(31.4,30.9)	(19.5,19.0)	(10.9,10.4)
	(36.3,35.8)	(19.1,18.6)	(14.1,13.6)	(9.9,9.4)	(6.3,5.8)	(263.5,263.0)	(216.2,215.7)	(191.4,190.9)	(161.1,160.6)	(123.9,123.4)
0.99	(182.9,182.4)	(182.4,181.9)	(182.0,181.5)	(181.6,181.1)	(180.8,180.3)	(212.4,211.9)	(207.0,206.5)	(203.9,203.4)	(199.5,199.0)	(192.9,192.4)
	(182.3,181.8)	(179.3,178.8)	(177.2,176.7)	(174.0,173.5)	(168.8,168.3)	(216.3,215.8)	(215.9,215.4)	(215.5,215.0)	(215.0,214.5)	(214.0,213.5)
1.01	(216.2,215.6)	(215.7,215.2)	(215.4,214.9)	(214.9,214.4)	(213.9,213.4)	(182.4,181.9)	(179.5,179.0)	(177.5,177.0)	(174.4,173.9)	(169.3,168.8)
	(212.3,211.8)	(207.0,206.5)	(203.9,203.4)	(199.7,199.2)	(193.1,192.6)	(183.1,182.6)	(182.5,182.0)	(182.2,181.7)	(181.8,181.3)	(181.0,180.5)
1.10	(267.6,267.1)	(225.4,224.9)	(202.6,202.1)	(173.9,173.4)	(137.5,137.0)	(43.4,42.9)	(23.9,23.4)	(18.0,17.4)	(12.7, 12.2)	(8.2,7.7)
	(130.8,130.3)	(57.1,56.5)	(39.0,38.5)	(24.9 24.4)	(14.3,13.8)	(66.3,65.8)	(58.5,58.0)	(54.2,53.7)	(48.5,48.0)	(40.9,40.4)
	$\rho_0 = \rho_1 = -0.4$									
0.90	(56.8,56.3)	(49.5,49.0)	(45.5,45.0)	(40.2,39.7)	(33.3, 32.8)	(115.0,114.5)	(44.4,43.9)	(28.8,28.3)	(17.5,17.0)	(9.5,9.0)
	(33.5, 33.0)	(17.0,16.5)	(12.4,11.8)	(8.5,8.0)	(5.4,4.9)	(264.0,263.5)	(216.1,215.6)	(191.1,190.6)	(160.6,160.1)	(123.3,122.8)
0.99	(182.5,182.0)	(182.0,181.5)	(181.7,181.2)	(181.3,180.8)	(180.5,180.0)	(213.2,212.7)	(207.6,207.1)	(204.2,203.7)	(199.5,199.0)	(192.1,191.6)
	(181.2,180.7)	(177.5,177.0)	(175.1,174.6)	(171.5,171.0)	(165.7,165.2)	(216.7,216.2)	(216.2,215.7)	(215.8,215.3)	(215.3,214.8)	(214.3,213.8)
1.01	(216.5,216.0)	(216.0,215.5)	(215.7,215.2)	(215.1,214.6)	(214.2,213.7)	(181.4,180.9)	(177.8,177.3)	(175.4,174.9)	(171.9,171.4)	(166.2,165.7)
	(213.1,212.6)	(207.6,207.1)	(204.3,203.8)	(199.6,199.1)	(192.4,191.9)	(182.7,182.2)	(182.2,181.7)	(181.9,181.4)	(181.5,181.0)	(180.7,180.2)
1.10	(268.3,267.8)	(225.5,225.0)	(202.4,201.9)	(173.4,172.9)	(136.9,136.4)	(40.3,39.8)	(21.4,20.9)	(15.8,15.3)	(11.0,10.5)	(7.0,6.5)
	(128.4,127.9)	(53.8,53.3)	(36.0,35.5)	(22.5,22.0)	(12.5,12.0)	(64.8,64.3)	(57.3,56.8)	(53.1,52.6)	(47.6,47.1)	(40.1,39.6)
	$\rho_0 = \rho_1 = 0.0$									
0.90	(55.7,55.2)	(48.6,48.1)	(44.7,44.2)	(39.5,39.0)	(32.8,32.3)	(112.8,112.3)	(41.9,41.4)	(26.7,26.2)	(15.8,15.3)	(8.4,7.9)
	(31.3,30.8)	(15.3,14.8)	(11.0,10.5)	(7.5,6.9)	(4.7, 4.2)	(264.4,263.9)	(216.0,215.5)	(190.9,190.4)	(160.2,159.7)	(122.8,122.3)
0.99	(182.2,181.7)	(181.8,181.3)	(181.5,181.0)	(181.0,180.5)	(180.2,179.7)	(213.9,213.4)	(208.2,207.7)	(204.6,204.1)	(199.4,198.9)	(191.3,190.8)
	(180.2,179.7)	(175.9,175.4)	(173.2,172.7)	(169.1,168.6)	(162.7,162.2)	(217.0,216.5)	(216.4,215.9)	(216.1,215.6)	(215.5,215.0)	(214.5,214.0)
1.01	(216.8,216.3)	(216.3,215.8)	(215.9,215.4)	(215.3,214.8)	(214.3,213.8)	(180.4,179.9)	(176.2,175.7)	(173.5,173.0)	(169.5,169.0)	(163.2,162.7)
	(213.8,213.3)	(208.2,207.7)	(204.6,204.1)	(199.6,199.1)	(191.6,191.1)	(182.4,181.9)	(182.0,181.5)	(181.2,181.2)	(181.2,180.7)	(180.4,179.9)
1.10	(268.9,268.4)	(225.5,225.0)	(202.2,201.7)	(173.1,172.6)	(136.4,135.9)	(37.8,37.3)	(19.3,18.8)	(14.1,13.6)	(9.7,9.2)	(6.1,5.6)
	(126.4,125.9)	(51.0,50.5)	(33.5,33.0)	(20.5,20.0)	(11.1,10.6)	(63.6,63.1)	(56.4,55.9)	(52.2,51.7)	(46.8,46.3)	(39.4,38.9)
	$\rho_0 = \rho_1 = 0.4$									
0.90	(54.5,54.0)	(47.7,47.2)	(43.9,43.3)	(38.8,38.3)	(32.2,31.7)	(110.6,110.1)	(39.3,38.8)	(24.5,24.0)	(14.1,13.6)	(7.3,6.8)
	(29.1,28.6)	(13.6,13.1)	(9.6,9.1)	(6.5,5.9)	(4.0,3.5)	(264.8,264.3)	(215.9,215.4)	(190.6,190.1)	(159.7,159.2)	(122.2,121.7)
0.99	(181.9,181.4)	(181.5,181.0)	(181.2,180.7)	(180.7,180.2)	(179.9,179.4)	(214.6,214.1)	(208.8,208.3)	(204.9,204.4)	(199.3,198.8)	(190.4,189.9)
	(179.1,178.6)	(174.1,173.6)	(170.9,170.4)	(166.3,165.8)	(159.1,158.6)	(217.3,216.8)	(216.7,216.2)	(216.3,215.8)	(215.7,215.2)	(214.7,214.2)
1.01	(217.1,216.6)	(216.5,216.0)	(216.1,215.6)	(215.6,215.1)	(214.5,214.0)	(179.3,178.8)	(174.4,173.9)	(171.2,170.7)	(166.7,166.2)	(159.7,159.1)
	(214.5,214.0)	(208.8,208.3)	(205.0,204.5)	(199.5,199.0)	(190.7,190.2)	(182.1,181.6)	(181.7,181.2)	(181.4,180.9)	(181.0,180.5)	(180.2,179.7)
1.10	(269.4,268.9)	(225.5,225.0)	(202.1,201.6)	(172.7,172.2)	(135.9,135.4)	(35.3,34.8)	(17.3,16.8)	(12.4,11.9)	(8.4, 7.9)	(5.2,4.7)
	(124.3,123.7)	(48.2,47.7)	(30.9,30.4)	(18.4,17.9)	(9.8,9.3)	(62.4,61.9)	(55.4,54.9)	(51.4,50.9)	(46.0,45.5)	(38.7,38.2)
	$\rho_0 = \rho_1 = 0.9$									
0.90	(53.0,52.5)	(46.6,46.1)	(42.8,42.3)	(37.9,37.4)	(31.4,30.9)	(107.7,107.2)	(36.0,35.5)	(21.7,21.2)	(12.1,11.5)	(6.0,5.5)
	(26.3,25.8)	(11.6,11.1)	(8.0,7.5)	(5.3,4.7)	(3.3,2.7)	(265.3,264.8)	(215.8,215.3)	(190.3,189.8)	(159.2,158.7)	(121.5,121.0)
0.99	(181.5,181.0)	(181.2,180.7)	(180.9,180.4)	(180.4,179.9)	(179.6,179.1)	(215.8,215.3)	(209.8,209.3)	(205.5,205.0)	(199.1,198.6)	(188.9,188.4)
	(177.6,177.1)	(171.3,170.8)	(167.4,166.9)	(161.9,161.4)	(153.5,153.0)	(217.7,217.2)	(217.0,216.5)	(216.6,216.1)	(216.0,215.5)	(214.9,214.4)
1.01	(217.5,217.0)	(216.9,216.4)	(216.5,216.0)	(215.8,215.3)	(214.8,214.3)	(177.8,177.3)	(171.7,171.2)	(167.8,167.3)	(162.4,161.9)	(154.1,153.6)
	(215.6,215.1)	(209.8,209.3)	(205.6,205.1)	(199.4,198.9)	(189.3,188.8)	(181.7,181.2)	(181.4,180.9)	(181.1,180.6)	(180.6,180.1)	(179.8,179.3)
1.10	(270.2,269.7)	(225.6,225.1)	(201.8,201.3)	(172.3,171.8)	(135.2,134.7)	(32.1,31.6)	(14.8,14.3)	(10.3,9.8)	(6.8,6.3)	(4.2,3.7)
	(121.4,120.9)	(44.4,43.9)	(27.6,27.1)	(15.8,15.3)	(8.1,7.6)	(60.8,60.3)	(54.2,53.7)	(50.3,49.8)	(45.0,44.5)	(37.9,37.4)

Table 7. The $(ARL_1, SDRRL_1)$ values of the Shewhart-RZ control chart in the presence of autocorrelation for $\Phi_{XX} = \Phi_{YY} = 0.1$ (first row), $\Phi_{XX} = \Phi_{YY} = 0.7$ (second row), $\gamma_X \in \{0.01, 0.2\}$, $\gamma_X \in \{0.01, 0.2\}$, $\gamma_X = \gamma_Y$, $(\rho_0, \rho_1) = \{(-0.4, -0.2), (-0.4, -0.9), (0.4, 0.2), (0.4, 0.9)\}$, $n \in \{2, 5, 7, 10, 15\}$ and $ARL_0 = 200$.

τ	$n = 2$	$n = 5$	$n = 7$	$n = 10$	$n = 15$	$\rho_0 = -0.4, \rho_1 = -0.2$	$n = 5$	$n = 10$	$n = 15$
0.90	(1.0,0.0)	(1.0,0.0)	(1.0,0.0)	(1.0,0.0)	(1.0,0.0)	(210.2,209.7)	(111.2,110.7)	(79.9,79.4)	(53.4,52.9)
0.95	(1.0,0.1)	(1.0,0.0)	(1.0,0.0)	(1.0,0.0)	(1.0,0.0)	(257.6,257.1)	(263.4,262.9)	(258.9,258.4)	(246.3,245.8)
0.99	(3.1,2.6)	(1.0,0.0)	(1.0,0.0)	(1.0,0.0)	(1.0,0.0)	(308.9,308.4)	(257.8,257.3)	(224.9,224.4)	(186.0,185.5)
1.01	(65.1,64.6)	(22.4,21.9)	(14.0,13.5)	(8.2,7.7)	(4.4,3.9)	(270.2,269.7)	(294.1,293.6)	(302.8,302.3)	(309.5,309.0)
1.05	(169.2,168.7)	(134.2,133.7)	(116.7,116.2)	(95.8,95.3)	(71.4,70.9)	(354.8,354.3)	(380.0,379.5)	(383.5,383.0)	(379.6,379.1)
1.10	(66.5,66.0)	(23.0,22.5)	(14.4,13.9)	(8.5,8.0)	(4.6,4.1)	(274.2,273.7)	(304.4,303.9)	(318.3,317.8)	(350.6,350.1)
1.01	(171.4,170.9)	(136.3,135.8)	(118.6,118.1)	(97.6,97.1)	(72.9,72.4)	(354.8,354.3)	(380.0,379.5)	(383.5,383.0)	(380.1,379.6)
1.05	(66.5,66.0)	(23.0,22.5)	(14.4,13.9)	(8.5,8.0)	(4.6,4.1)	(274.2,273.7)	(304.4,303.9)	(318.3,317.8)	(350.6,350.1)
1.10	(171.4,170.9)	(136.3,135.8)	(118.6,118.1)	(97.6,97.1)	(72.9,72.4)	(354.8,354.3)	(380.0,379.5)	(383.5,383.0)	(380.1,379.6)
1.01	(66.5,66.0)	(23.0,22.5)	(14.4,13.9)	(8.5,8.0)	(4.6,4.1)	(274.2,273.7)	(304.4,303.9)	(318.3,317.8)	(350.6,350.1)
1.05	(171.4,170.9)	(136.3,135.8)	(118.6,118.1)	(97.6,97.1)	(72.9,72.4)	(354.8,354.3)	(380.0,379.5)	(383.5,383.0)	(380.1,379.6)
1.10	(66.5,66.0)	(23.0,22.5)	(14.4,13.9)	(8.5,8.0)	(4.6,4.1)	(274.2,273.7)	(304.4,303.9)	(318.3,317.8)	(350.6,350.1)
1.01	(171.4,170.9)	(136.3,135.8)	(118.6,118.1)	(97.6,97.1)	(72.9,72.4)	(354.8,354.3)	(380.0,379.5)	(383.5,383.0)	(380.1,379.6)
1.05	(66.5,66.0)	(23.0,22.5)	(14.4,13.9)	(8.5,8.0)	(4.6,4.1)	(274.2,273.7)	(304.4,303.9)	(318.3,317.8)	(350.6,350.1)
1.10	(171.4,170.9)	(136.3,135.8)	(118.6,118.1)	(97.6,97.1)	(72.9,72.4)	(354.8,354.3)	(380.0,379.5)	(383.5,383.0)	(380.1,379.6)
0.90	(1.0,0.0)	(1.0,0.0)	(1.0,0.0)	(1.0,0.0)	(1.0,0.0)	(260.6,260.1)	(270.2,269.7)	(268.4,267.9)	(236.7,236.2)
0.95	(1.0,0.0)	(1.0,0.0)	(1.0,0.0)	(1.0,0.0)	(1.0,0.0)	(61.9,61.4)	(37.6,37.1)	(29.8,29.3)	(22.4,21.9)
0.99	(1.1,0.4)	(1.0,0.0)	(1.0,0.0)	(1.0,0.0)	(1.0,0.0)	(79.2,78.7)	(116.8,116.3)	(94.3,93.8)	(50.9,50.4)
1.01	(25.3,24.8)	(12.1,11.6)	(8.6,8.1)	(5.9,5.3)	(3.7,3.2)	(86.2,85.7)	(103.3,102.8)	(97.8,97.3)	(87.9,87.4)
1.05	(46.8,46.3)	(40.6,40.1)	(37.2,36.7)	(32.3,31.8)	(27.3,26.8)	(86.2,85.7)	(103.3,102.8)	(97.8,97.3)	(87.9,87.4)
1.10	(47.2,46.7)	(41.0,40.5)	(37.6,37.1)	(33.1,32.6)	(27.3,26.8)	(86.2,85.7)	(103.3,102.8)	(97.8,97.3)	(87.9,87.4)
0.90	(1.0,0.0)	(1.0,0.0)	(1.0,0.0)	(1.0,0.0)	(1.0,0.0)	(111.5,111.0)	(92.0,91.5)	(83.9,83.4)	(75.0,74.5)
0.95	(1.1,0.4)	(1.0,0.0)	(1.0,0.0)	(1.0,0.0)	(1.0,0.0)	(79.2,78.7)	(116.8,116.3)	(94.3,93.8)	(50.9,50.4)
0.99	(2.8,2.3)	(2.0,1.4)	(1.7,1.1)	(1.4,0.8)	(1.2,0.5)	(86.2,85.7)	(103.3,102.8)	(97.8,97.3)	(87.9,87.4)
1.01	(25.3,24.8)	(12.1,11.6)	(8.6,8.1)	(5.9,5.3)	(3.7,3.2)	(86.2,85.7)	(103.3,102.8)	(97.8,97.3)	(87.9,87.4)
1.05	(46.8,46.3)	(40.6,40.1)	(37.2,36.7)	(32.3,31.8)	(27.3,26.8)	(86.2,85.7)	(103.3,102.8)	(97.8,97.3)	(87.9,87.4)
1.10	(47.2,46.7)	(41.0,40.5)	(37.6,37.1)	(33.1,32.6)	(27.3,26.8)	(86.2,85.7)	(103.3,102.8)	(97.8,97.3)	(87.9,87.4)
0.90	(1.0,0.0)	(1.0,0.0)	(1.0,0.0)	(1.0,0.0)	(1.0,0.0)	(117.0,116.5)	(100.8,100.3)	(94.6,94.1)	(88.3,87.8)
0.95	(1.1,0.4)	(1.0,0.0)	(1.0,0.0)	(1.0,0.0)	(1.0,0.0)	(65.4,64.9)	(41.9,41.4)	(33.9,33.4)	(26.2,25.7)
0.99	(4.7,4.2)	(3.3,2.7)	(3.2,2.7)	(2.8,2.3)	(2.2,1.7)	(112.7,112.2)	(93.9,93.4)	(86.2,85.7)	(77.8,77.3)
1.01	(27.9,27.4)	(22.4,21.9)	(19.7,19.2)	(16.4,15.9)	(12.6,12.1)	(109.8,109.3)	(94.1,93.6)	(88.6,88.1)	(83.2,82.7)
1.05	(48.4,47.9)	(41.0,40.5)	(37.6,37.1)	(33.1,32.6)	(27.3,26.8)	(117.0,116.5)	(100.8,100.3)	(94.6,94.1)	(88.3,87.8)
1.10	(47.2,46.7)	(41.0,40.5)	(37.6,37.1)	(33.1,32.6)	(27.3,26.8)	(117.0,116.5)	(100.8,100.3)	(94.6,94.1)	(88.3,87.8)
0.90	(1.0,0.0)	(1.0,0.0)	(1.0,0.0)	(1.0,0.0)	(1.0,0.0)	(41.6,41.1)	(19.7,19.2)	(14.2,13.7)	(9.8,9.3)
0.95	(1.0,0.0)	(1.0,0.0)	(1.0,0.0)	(1.0,0.0)	(1.0,0.0)	(98.6,98.1)	(75.7,75.2)	(66.3,65.8)	(56.0,55.5)
0.99	(1.3,0.6)	(1.0,0.0)	(1.0,0.0)	(1.0,0.0)	(1.0,0.0)	(64.9,64.4)	(45.8,45.3)	(38.9,38.3)	(31.6,31.1)
1.01	(4.7,4.2)	(3.3,2.7)	(3.2,2.7)	(2.8,2.3)	(2.2,1.7)	(107.0,106.5)	(89.3,88.8)	(82.4,81.9)	(75.2,74.7)
1.05	(28.3,27.8)	(22.8,22.3)	(20.0,19.5)	(16.7,16.2)	(12.8,12.3)	(109.8,109.3)	(94.1,93.6)	(88.6,88.1)	(83.2,82.7)
1.10	(47.2,46.7)	(41.0,40.5)	(37.6,37.1)	(33.1,32.6)	(27.3,26.8)	(117.0,116.5)	(100.8,100.3)	(94.6,94.1)	(88.3,87.8)
0.90	(1.0,0.0)	(1.0,0.0)	(1.0,0.0)	(1.0,0.0)	(1.0,0.0)	(543.9,543.9)	(1296.8,1296.3)	(516.9,516.4)	(42.3, 41.8)
0.95	(1.0,0.0)	(1.0,0.0)	(1.0,0.0)	(1.0,0.0)	(1.0,0.0)	(1352.2,1351.7)	(3043.2,3042.7)	(4174.9,4174.4)	(5658.7,5658.2)
0.99	(1.1,0.3)	(1.0,0.0)	(1.0,0.0)	(1.0,0.0)	(1.0,0.0)	(1906.8,1906.3)	(2052.9,2052.4)	(1424.5,1424.0)	(332.1,332.0)
1.01	(316.1,315.6)	(18.2,17.7)	(6.5,6.0)	(2.6,2.0)	(1.3,0.6)	(1432.4,1431.9)	(3757.5,3757.0)	(6002.4,6001.9)	(10119.0,10118.5)
1.05	(7057.5,7057.0)	(314.0,313.5)	(196.4,196.3)	(103.9,103.8)	(41.7,41.6)	(3398.2,3398.1)	(4013.3,4012.8)	(6765.7,6765.2)	(245290.2,245289.7)
1.10	(7399.8,7399.3)	(331.0,330.5)	(207.6,207.5)	(110.2,110.1)	(44.4,44.3)	(3400.1,3400.0)	(4198.3,4198.2)	(6766.3,6765.8)	(262343.7,262343.2)
1.01	(66.5,66.0)	(23.0,22.5)	(14.4,13.9)	(8.5,8.0)	(4.6,4.1)	(274.2,273.7)	(304.4,303.9)	(318.3,317.8)	(27672.4,27671.9)
1.05	(171.4,170.9)	(136.3,135.8)	(118.6,118.1)	(97.6,97.1)	(72.9,72.4)	(354.8,354.3)	(380.0,379.5)	(383.5,383.0)	(4237.6,4237.1)
1.10	(66.5,66.0)	(23.0,22.5)	(14.4,13.9)	(8.5,8.0)	(4.6,4.1)	(274.2,273.7)	(304.4,303.9)	(318.3,317.8)	(350.6,350.1)
1.01	(171.4,170.9)	(136.3,135.8)	(118.6,118.1)	(97.6,97.1)	(72.9,72.4)	(354.8,354.3)	(380.0,379.5)	(383.5,383.0)	(380.1,379.6)
1.05	(66.5,66.0)	(23.0,22.5)	(14.4,13.9)	(8.5,8.0)	(4.6,4.1)	(274.2,273.7)	(304.4,303.9)	(318.3,317.8)	(350.6,350.1)
1.10	(171.4,170.9)	(136.3,135.8)	(118.6,118.1)	(97.6,97.1)	(72.9,72.4)	(354.8,354.3)	(380.0,379.5)	(383.5,383.0)	(380.1,379.6)
1.01	(66.5,66.0)	(23.0,22.5)	(14.4,13.9)	(8.5,8.0)	(4.6,4.1)	(274.2,273.7)	(304.4,303.9)	(318.3,317.8)	(350.6,350.1)
1.05	(171.4,170.9)	(136.3,135.8)	(118.6,118.1)	(97.6,97.1)	(72.9,72.4)	(354.8,354.3)	(380.0,379.5)	(383.5,383.0)	(380.1,379.6)
1.10	(66.5,66.0)	(23.0,22.5)	(14.4,13.9)	(8.5,8.0)	(4.6,4.1)	(274.2,273.7)	(304.4,303.9)	(318.3,317.8)	(350.6,350.1)
1.01	(171.4,170.9)	(136.3,135.8)	(118.6,118.1)	(97.6,97.1)	(72.9,72.4)	(354.8,354.3)	(380.0,379.5)	(383.5,383.0)	(380.1,379.6)
1.05	(66.5,66.0)	(23.0,22.5)	(14.4,13.9)	(8.5,8.0)	(4.6,4.1)	(274.2,273.7)	(304.4,303.9)	(318.3,317.8)	(350.6,350.1)
1.10	(171.4,170.9)	(136.3,135.8)	(118.6,118.1)	(97.6,97.1)	(72.9,72.4)	(354.8,354.3)	(380.0,379.5)	(383.5,383.0)	(380.1,379.6)
1.01	(66.5,66.0)	(23.0,22.5)	(14.4,13.9)	(8.5,8.0)	(4.6,4.1)	(274.2,273.7)	(304.4,303.9)	(318.3,317.8)	(350.6,350.1)
1.05	(171.4,170.9)	(136.3,135.8)	(118.6,118.1)	(97.6,97.1)	(72.9,72.4)	(354.8,354.3)	(380.0,379.5)	(383.5,383.0)	(380.1,379.6)
1.10	(66.5,66.0)	(23.0,22.5)	(14.4,13.9)	(8.5,8.0)	(4.6,4.1)	(274.2,273.7)	(304.4,303.9)	(318.3,317.8)	(350.6,350.1)
1.01	(171.4,170.9)	(136.3,135.8)	(118.6,118.1)	(97.6,97.1)	(72.9,72.4)	(354.8,354.3)	(380.0,379.5)	(383.5,383.0)	(380.1,379.6)
1.05	(66.5,66.0)	(23.0,22.5)	(14.4,13.9)	(8.5,8.0)	(4.6,4.1)	(274.2,273.7)	(304.4,303.9)	(318.3,317.8)	(350.6,350.1)
1.10	(171.4,170.9)	(136.3,135.8)	(118.6,118.1)	(97.6,97.1)	(72.9,72.4)	(354.8,354.3)	(380.0,379.5)	(383.5,383.0)	(380.1,379.6)
1.01	(66.5,66.0)	(23.0,22.5)	(14.4,13.9)	(8.5,8.0)	(4.6,4.1)	(274.2,273.7)	(304.4,303.9)	(318.3,317.8)	(350.6,350.1)
1.05	(171.4,170.9)	(136.3,135.8)	(118.6,118.1)	(97.6,97.1)	(72.9,72.4)	(354.8,354.3)	(380.0,379.5)	(383.5,383.0)	(380.1,379.6)
1.10	(66.5,66.0)	(23.0,22.5)	(14.4,13.9)	(8.5,8.0)	(4.6,4.1)	(274.2,273.7)	(304.4,303.9)	(318.3,317.8)	(350.6,350.1)
1.01	(171.4,170.9)	(136.3,135.8)	(118.6,118.1)	(97.6,97.1)	(72.9,72.4)	(354.8,354.3)	(380.0,379.5)	(383.5,383.0)	(380.1,379.6)
1.05	(66.5,66.0)	(23.0,22.5)	(14.4,13.9)	(8.5,8.0)	(4.6,4.1)	(274.2,273.7)	(304.4,303.9)	(318.3,317.8)	(350.6,350.1)
1.10	(171.4,170.9)	(136.3,135.8)	(118.6,118.1)	(97.6,97.1)	(72.9,72.4)	(354.8,354.3)	(380.0,379.5)	(383.5,383.0)	(380.1,379.6)
1.01	(66.5,66.0)	(23.0,22.5)	(14.4,13.9)	(8.5,8.0)	(4.6,4.1)	(274.2,273.7)	(304.4,303.9)	(318.3,317.8)	(350.6,350.1)
1.05	(171.4,170.9)	(136.3,135.8)	(118.6,118.1)	(97.6,97.1)	(72.9,72.4)	(354.8,354.3)	(380.0,379.5)	(383.5,383.0)	(380.1,379.6)
1.10	(66.5,66.0)	(23.0,22.5)	(14.4,13.9)	(8.5,8.0)	(4.6,4.1)	(274.2,273.7)	(304.4,303.9)	(318.3,317.8)	(350.6,350.1)
1.01	(171.4,170.9)	(136.3,135.8)	(118.6,118.1)	(97.6,97.1)	(72.9,72.4)	(354.8,354.3)	(380.0,379.5)	(383.5,383.0)	(380.1,379.6)
1.05	(66.5,66.0)	(23.0,22.5)	(14.4,13.9)	(8.5,8.0)	(4.6,4.1)	(274.2,273.7)	(304.4,303.9)	(318.3,317.8)	(350.6,350.1)
1.10	(171.4,170.9)	(136.3,135.8)	(118.6,118.1)	(97.6,97.1)	(72.9,72.4)	(354.8,354.3)	(380.0,379.5)	(383.5,383.0)	(380.1,379.6)
1.01	(66.5,66.0)	(23.0,22.5)	(14.4,13.9)	(8.5,8.0)	(4.6,4.1)	(274.2,273.7)	(304.4,303.9)	(318.3,317.8)	

Table 8. The $(ARL_1, SDRRL_1)$ values of the Shewhart-RZ control chart in the presence of autocorrelation for $\Phi_{XX} = \Phi_{YY} = 0.1$ (first row), $\Phi_{XX} = \Phi_{YY} = 0.7$ (second row), $\gamma_X \in \{0.01, 0.2\}$, $\gamma_X \in \{0.01, 0.2\}$, $\gamma_X \neq \gamma_Y$, $(\rho_0, \rho_1) \in \{(-0.4, -0.2), (-0.4, -0.9), (0.4, 0.2), (0.4, 0.9)\}$, $n \in \{2, 5, 7, 10, 15\}$ and $ARL_0 = 200$.

τ	$(\gamma_X = 0.01, \gamma_Y = 0.2)$					$(\gamma_X = 0.2, \gamma_Y = 0.01)$				
	$n = 2$	$n = 5$	$n = 10$	$n = 15$	$n = 2$	$n = 5$	$n = 7$	$n = 10$	$n = 15$	
0.90	(34.4, 33.9)	(16.4, 15.9)	(11.7, 11.1)	(7.9, 7.3)	(4.9, 4.4)	(119.3, 118.8)	(44.6, 44.1)	(28.4, 27.9)	(16.8, 16.3)	(8.9, 8.3)
	(63.1, 62.6)	(54.9, 54.4)	(50.3, 49.8)	(44.4, 43.9)	(36.6, 36.1)	(272.9, 272.4)	(224.6, 224.1)	(199.3, 198.8)	(168.0, 167.5)	(129.6, 129.1)
	(99.6, 99.1)	(67.7, 67.2)	(55.0, 54.5)	(42.3, 41.8)	(29.7, 29.2)	(207.5, 207.0)	(131.7, 131.2)	(103.5, 103.0)	(76.5, 76.0)	(51.0, 50.5)
	(127.2, 126.7)	(121.0, 120.5)	(117.0, 116.5)	(111.3, 110.8)	(102.4, 101.9)	(278.8, 278.3)	(262.3, 261.8)	(251.9, 251.4)	(237.0, 236.5)	(214.6, 214.1)
	(197.2, 196.7)	(192.3, 191.8)	(189.2, 188.7)	(184.6, 184.1)	(177.4, 176.9)	(231.3, 230.8)	(225.4, 224.9)	(221.5, 221.0)	(215.9, 215.4)	(207.2, 206.7)
0.99	(199.4, 198.9)	(199.1, 198.6)	(198.8, 198.3)	(198.3, 197.8)	(197.5, 197.0)	(234.6, 233.1)	(233.6, 233.1)	(233.2, 232.7)	(232.7, 232.2)	(231.7, 231.2)
	(231.2, 230.7)	(225.4, 224.9)	(221.6, 221.1)	(216.1, 215.6)	(207.5, 207.0)	(197.4, 196.9)	(192.6, 192.1)	(189.5, 189.0)	(185.1, 184.6)	(178.0, 177.5)
	(233.9, 233.4)	(233.4, 232.9)	(233.1, 232.6)	(232.5, 232.0)	(231.6, 231.1)	(199.6, 199.1)	(199.2, 198.7)	(199.0, 198.5)	(198.5, 198.0)	(197.7, 197.2)
	(211.5, 211.0)	(138.2, 137.7)	(110.1, 109.6)	(82.5, 82.0)	(55.9, 55.4)	(104.6, 104.1)	(72.8, 72.3)	(46.5, 46.0)	(33.1, 32.5)	
	(277.4, 276.9)	(262.4, 261.9)	(252.8, 252.3)	(239.1, 238.6)	(218.1, 217.6)	(131.1, 130.6)	(125.2, 124.7)	(121.5, 121.0)	(116.0, 115.5)	(107.4, 106.9)
1.10	(133.6, 133.1)	(54.4, 53.9)	(35.7, 35.2)	(21.8, 21.2)	(11.8, 11.3)	(41.6, 41.1)	(20.8, 20.3)	(15.0, 14.5)	(10.2, 9.7)	(6.4, 5.9)
	(277.9, 277.4)	(234.7, 234.2)	(211.2, 210.7)	(181.6, 181.1)	(144.0, 143.5)	(72.0, 71.5)	(63.6, 63.1)	(58.9, 58.4)	(52.6, 52.1)	(44.1, 43.6)
	(29.5, 29.0)	(14.9, 14.4)	(10.8, 10.3)	(7.4, 6.9)	(4.7, 4.2)	(105.4, 104.9)	(40.0, 39.5)	(25.8, 25.3)	(15.5, 15.0)	(8.4, 7.9)
	(50.7, 50.2)	(44.9, 44.4)	(41.6, 41.1)	(37.2, 36.7)	(31.2, 30.7)	(244.3, 243.8)	(199.9, 199.4)	(176.8, 176.3)	(148.7, 148.2)	(114.5, 114.0)
	(79.4, 78.9)	(56.1, 55.6)	(46.5, 46.0)	(36.4, 35.9)	(26.2, 25.7)	(175.2, 174.7)	(112.6, 112.1)	(89.2, 88.7)	(66.5, 66.0)	(45.0, 44.5)
0.99	(98.4, 97.9)	(94.2, 93.7)	(91.5, 91.0)	(87.6, 87.1)	(81.4, 80.9)	(233.4, 232.9)	(220.0, 219.5)	(211.5, 211.0)	(199.4, 198.9)	(181.0, 180.5)
	(153.2, 152.7)	(149.8, 149.3)	(147.6, 147.1)	(144.5, 144.0)	(139.4, 138.9)	(182.9, 182.4)	(178.6, 178.1)	(175.8, 175.3)	(171.8, 171.3)	(165.4, 164.9)
	(154.8, 154.3)	(154.5, 154.0)	(154.3, 153.8)	(154.0, 153.5)	(153.4, 152.9)	(184.9, 184.4)	(184.6, 184.1)	(184.3, 183.8)	(183.9, 183.4)	(183.2, 182.7)
	(182.8, 182.3)	(178.6, 178.1)	(175.9, 175.4)	(171.9, 171.4)	(165.6, 165.1)	(153.4, 152.9)	(150.1, 149.6)	(147.9, 147.4)	(144.8, 144.3)	(139.8, 139.3)
	(184.8, 184.3)	(184.4, 183.9)	(184.2, 183.7)	(183.8, 183.3)	(183.1, 182.6)	(155.0, 154.5)	(154.7, 154.2)	(154.5, 154.0)	(154.2, 153.7)	(153.6, 153.1)
1.05	(177.9, 177.4)	(117.8, 117.3)	(94.5, 94.0)	(71.5, 71.0)	(49.2, 48.7)	(83.1, 82.6)	(60.0, 59.5)	(50.2, 49.7)	(39.8, 39.3)	(29.0, 28.5)
	(231.4, 230.9)	(219.2, 218.7)	(211.5, 211.0)	(200.4, 199.9)	(183.3, 182.8)	(101.4, 100.9)	(97.4, 96.9)	(94.8, 94.3)	(91.0, 90.5)	(85.0, 84.5)
	(117.5, 117.0)	(48.4, 47.9)	(32.2, 31.7)	(19.9, 19.4)	(11.0, 10.5)	(35.2, 34.7)	(18.6, 18.1)	(13.7, 13.2)	(9.5, 9.0)	(6.1, 5.6)
	(246.5, 246.0)	(207.3, 206.8)	(186.2, 185.7)	(159.8, 159.3)	(126.5, 126.0)	(57.4, 56.9)	(51.5, 51.0)	(48.1, 47.6)	(43.5, 43.0)	(37.1, 36.6)
	(27.8, 27.3)	(13.7, 13.2)	(9.8, 9.3)	(6.7, 6.2)	(4.3, 3.7)	(106.5, 106.0)	(38.9, 38.4)	(24.6, 24.1)	(14.5, 14.0)	(7.7, 7.2)
0.95	(49.3, 48.8)	(43.3, 42.8)	(39.9, 39.4)	(35.4, 34.9)	(29.5, 29.0)	(255.3, 254.8)	(207.1, 206.6)	(182.3, 181.8)	(152.3, 151.8)	(116.0, 115.5)
	(80.1, 79.6)	(55.2, 54.7)	(45.1, 44.6)	(34.9, 34.4)	(24.7, 24.2)	(184.0, 183.5)	(114.9, 114.4)	(89.8, 89.3)	(66.0, 65.5)	(43.8, 43.3)
	(101.2, 100.7)	(96.5, 96.0)	(93.4, 92.9)	(89.1, 88.6)	(82.2, 81.7)	(251.1, 250.6)	(235.4, 234.9)	(225.5, 225.0)	(211.6, 211.1)	(190.6, 190.1)
	(163.5, 163.0)	(159.5, 159.0)	(156.9, 156.4)	(153.2, 152.7)	(147.2, 146.7)	(197.1, 196.6)	(192.0, 191.5)	(188.7, 188.2)	(183.8, 183.3)	(176.3, 175.8)
	(165.4, 164.9)	(165.1, 164.6)	(164.8, 164.3)	(164.4, 163.9)	(163.7, 163.2)	(199.5, 199.0)	(199.1, 198.6)	(198.8, 198.3)	(198.3, 197.8)	(197.5, 197.0)
1.01	(197.0, 196.5)	(192.0, 191.5)	(188.7, 188.2)	(184.0, 183.5)	(176.6, 176.1)	(163.7, 163.2)	(159.8, 159.3)	(157.2, 156.7)	(153.5, 153.0)	(147.7, 147.2)
	(199.4, 198.9)	(199.0, 198.5)	(198.7, 198.2)	(198.2, 197.7)	(197.3, 196.8)	(165.6, 165.1)	(165.3, 164.7)	(165.0, 164.5)	(164.6, 164.1)	(164.0, 163.5)
	(187.3, 186.8)	(120.5, 120.0)	(95.5, 95.0)	(71.2, 70.7)	(48.0, 47.5)	(84.1, 83.6)	(59.2, 58.7)	(48.9, 48.4)	(38.3, 37.8)	(27.5, 27.0)
	(249.2, 248.7)	(234.9, 234.4)	(225.9, 225.4)	(213.0, 212.5)	(193.5, 193.0)	(104.5, 104.0)	(100.0, 99.5)	(97.1, 96.6)	(92.9, 92.4)	(86.3, 85.8)
	(119.3, 118.8)	(47.4, 46.9)	(30.9, 30.4)	(18.8, 18.3)	(10.2, 9.7)	(33.6, 33.1)	(17.2, 16.7)	(12.6, 12.1)	(8.7, 8.2)	(5.5, 5.0)
1.10	(259.1, 258.5)	(216.0, 215.5)	(193.0, 192.5)	(164.5, 164.0)	(128.9, 128.4)	(56.4, 55.9)	(50.2, 49.7)	(46.6, 46.1)	(41.9, 41.4)	(35.4, 34.9)
	(32.9, 32.4)	(15.1, 14.6)	(10.7, 10.1)	(7.1, 6.6)	(4.4, 3.9)	(121.6, 121.1)	(43.7, 43.2)	(27.3, 26.8)	(15.8, 15.3)	(8.2, 7.6)
	(63.1, 62.6)	(54.2, 53.7)	(49.3, 48.8)	(43.1, 42.6)	(35.1, 34.6)	(284.7, 284.2)	(233.5, 233.0)	(206.5, 206.0)	(173.3, 172.8)	(132.5, 132.0)
	(103.5, 102.9)	(67.9, 67.4)	(54.4, 53.9)	(41.1, 40.6)	(28.3, 27.8)	(220.4, 219.9)	(136.1, 135.6)	(105.6, 105.1)	(76.8, 76.3)	(50.2, 49.7)
	(135.9, 135.4)	(128.4, 127.9)	(123.7, 123.2)	(117.0, 116.5)	(106.7, 106.2)	(301.8, 301.3)	(282.8, 282.3)	(271.0, 270.5)	(254.0, 253.5)	(228.4, 227.9)
0.99	(217.6, 217.1)	(211.6, 211.1)	(207.7, 207.2)	(202.0, 201.5)	(193.2, 192.7)	(255.9, 255.4)	(248.6, 248.1)	(243.9, 243.4)	(237.1, 236.6)	(226.4, 225.9)
	(220.2, 219.7)	(219.8, 219.3)	(219.5, 219.0)	(218.9, 218.4)	(217.9, 217.4)	(258.9, 258.4)	(258.5, 258.0)	(258.1, 257.6)	(257.5, 257.0)	(256.3, 255.8)
	(255.8, 255.3)	(248.7, 248.2)	(244.0, 243.5)	(237.3, 236.8)	(226.8, 226.3)	(217.8, 217.3)	(212.0, 211.5)	(208.1, 207.6)	(202.6, 202.1)	(193.9, 193.4)
	(258.7, 258.2)	(258.3, 257.8)	(258.0, 257.5)	(257.4, 256.9)	(256.2, 255.7)	(220.4, 219.9)	(220.0, 219.5)	(219.7, 219.2)	(219.2, 218.7)	(218.2, 217.7)
	(225.2, 224.7)	(143.3, 142.8)	(112.7, 112.2)	(83.2, 82.7)	(55.3, 54.8)	(109.1, 108.6)	(73.4, 72.9)	(59.4, 58.9)	(45.4, 44.9)	(31.7, 31.2)
1.05	(300.8, 300.3)	(283.6, 283.1)	(272.6, 272.1)	(256.8, 256.3)	(232.8, 232.3)	(140.5, 140.0)	(133.4, 132.9)	(128.9, 128.4)	(122.4, 121.9)	(112.3, 111.8)
	(137.0, 136.5)	(53.7, 53.2)	(34.6, 34.1)	(20.7, 20.2)	(10.9, 10.4)	(40.3, 39.8)	(19.4, 18.9)	(13.8, 13.3)	(9.3, 8.8)	(5.8, 5.2)
	(291.6, 291.1)	(245.2, 244.7)	(220.0, 219.5)	(188.3, 187.8)	(148.0, 147.5)	(72.9, 72.4)	(63.6, 63.1)	(58.5, 58.0)	(51.7, 51.2)	(42.8, 42.3)

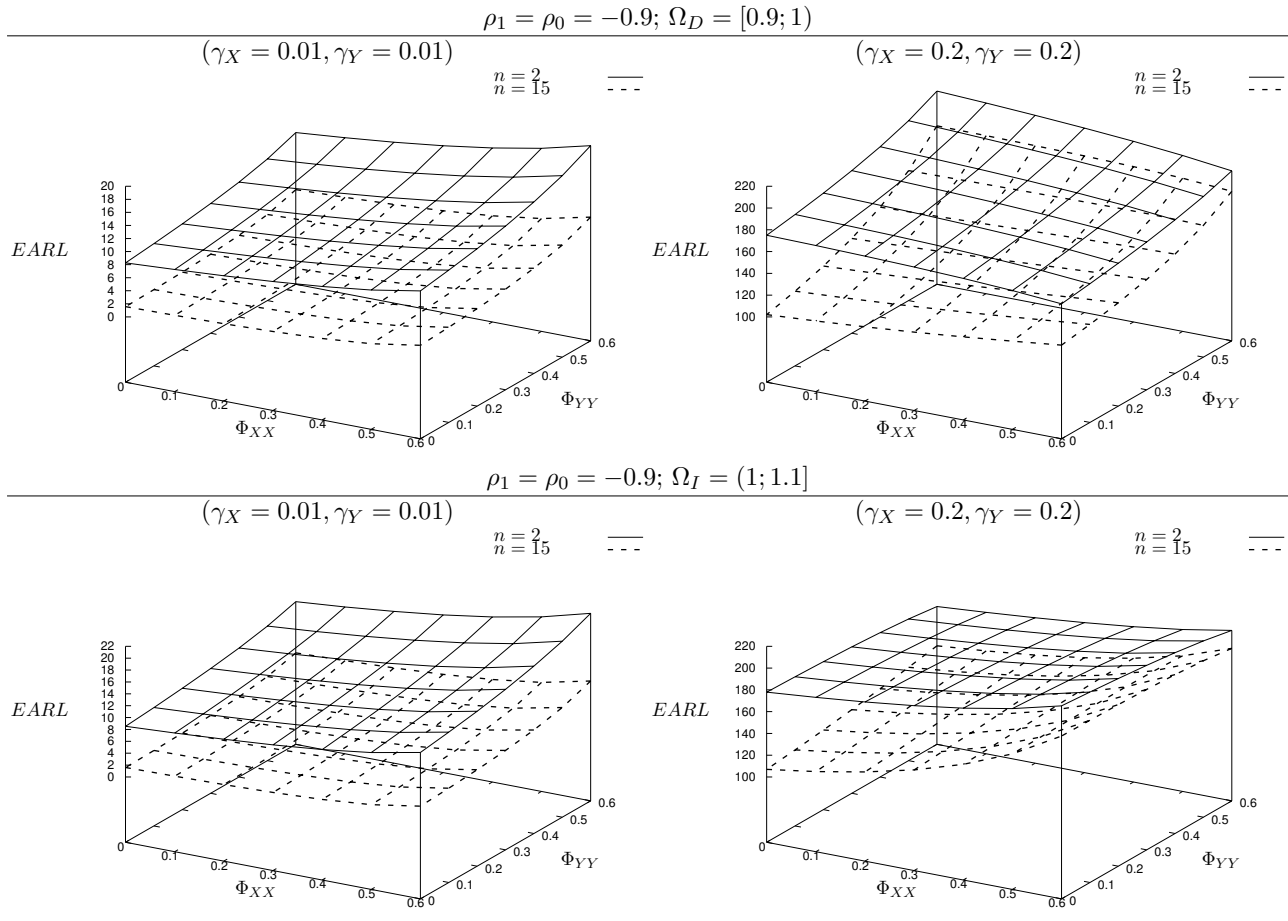


Figure 1. The effects of Φ_{XX} and Φ_{YY} on the overall performance of the Shewhart-RZ control chart in the presence of autocorrelation for $n \in \{2, 15\}$, $\gamma_X \in \{0.01, 0.2\}$, $\gamma_Y \in \{0.01, 0.2\}$, $\gamma_X = \gamma_Y$, $\rho_0 = \rho_1 = -0.9$ and $ARL_0 = 200$.

Alt Text: This figure illustrates the surface plots of $EARL$ against the coefficients Φ_{XX} and Φ_{YY} .

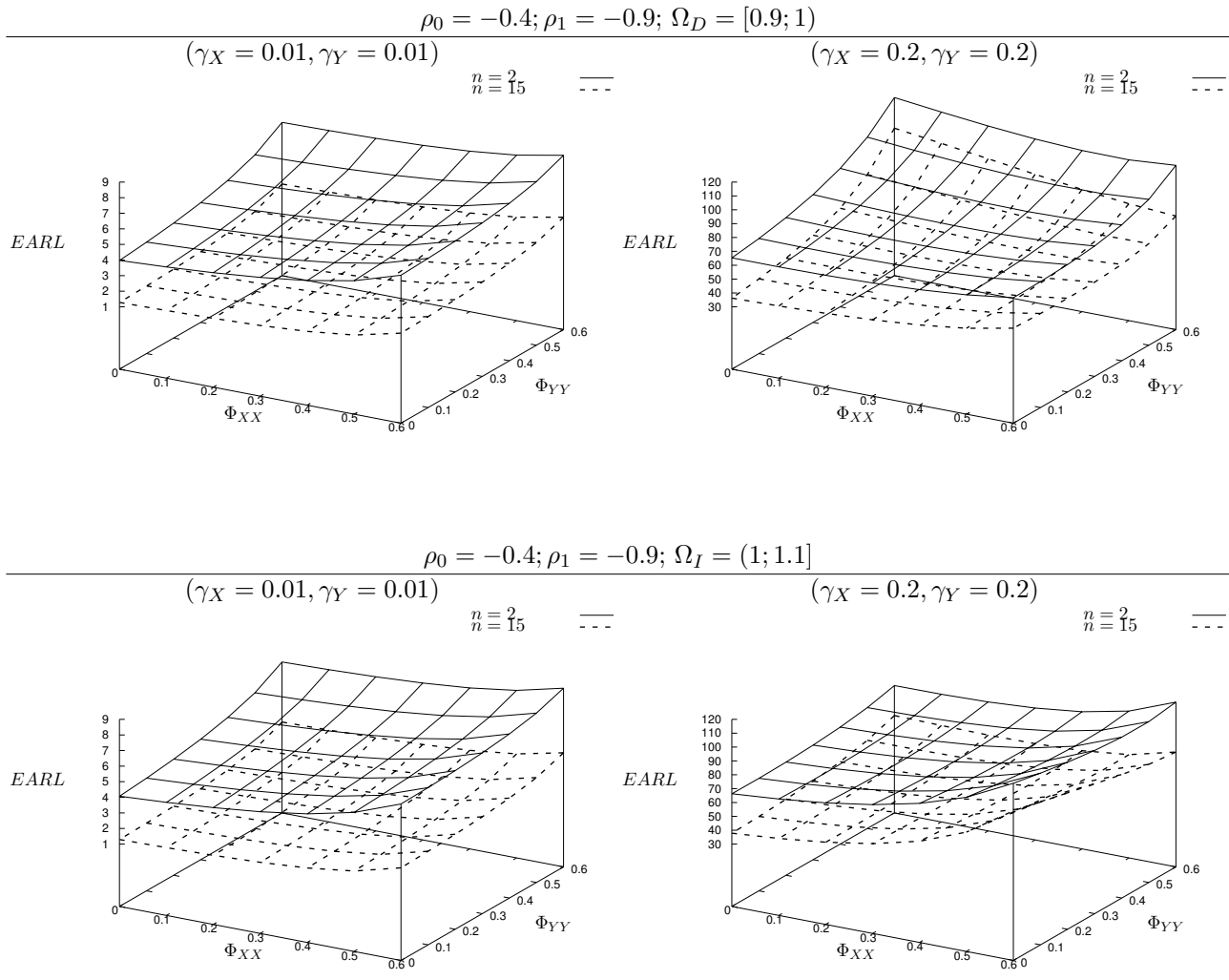
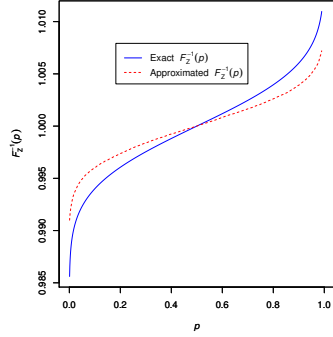
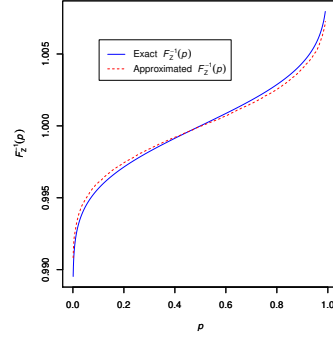


Figure 2. The effects of Φ_{XX} and Φ_{YY} on the overall performance of the Shewhart-RZ control chart in the presence of autocorrelation for $n \in \{2, 15\}$, $\gamma_X \in \{0.01, 0.2\}$, $\gamma_Y \in \{0.01, 0.2\}$, $\gamma_X = \gamma_Y$, $\rho_0 = -0.4$, $\rho_1 = -0.9$ and $ARL_0 = 200$.

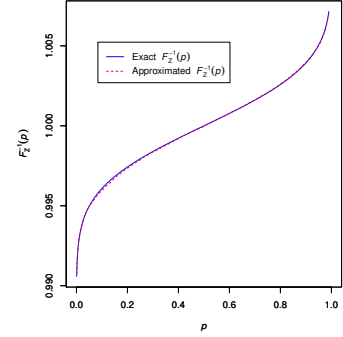
Alt Text: This figure illustrates the surface plots of $EARL$ against the coefficients Φ_{XX} and Φ_{YY} .



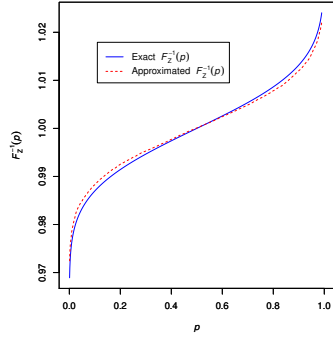
(a) $n = 2, \gamma_X = \gamma_Y = 0.01, \rho = 0.9, \Phi_{XX} = \Phi_{YY} = 0.1.$



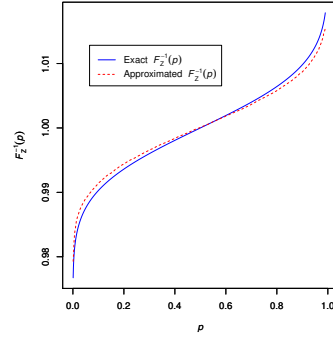
(b) $n = 4, \gamma_X = \gamma_Y = 0.01, \rho = 0.9, \Phi_{XX} = \Phi_{YY} = 0.1.$



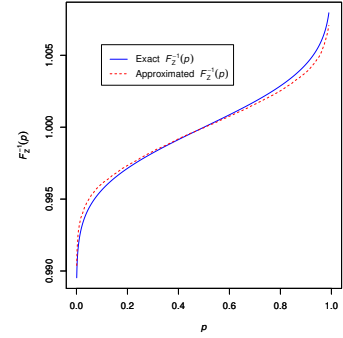
(c) $n = 5, \gamma_X = \gamma_Y = 0.01, \rho = 0.9, \Phi_{XX} = \Phi_{YY} = 0.1.$



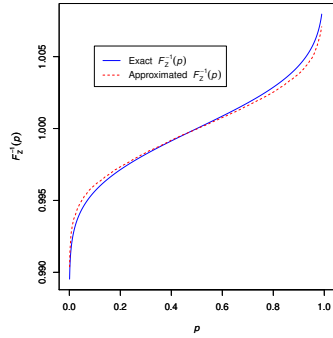
(d) $\rho = -0.9, n = 4, \gamma_X = \gamma_Y = 0.01, \Phi_{XX} = \Phi_{YY} = 0.1$



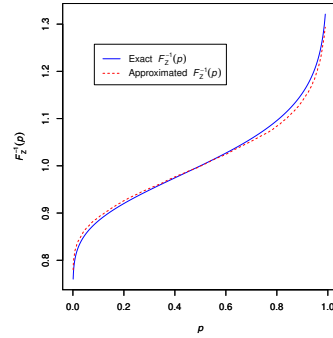
(e) $\rho = 0, n = 4, \gamma_X = \gamma_Y = 0.01, \Phi_{XX} = \Phi_{YY} = 0.1$



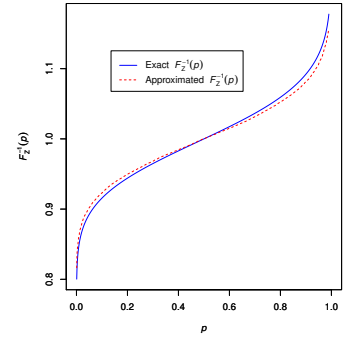
(f) $\rho = 0.9, n = 4, \gamma_X = \gamma_Y = 0.01, \Phi_{XX} = \Phi_{YY} = 0.1$



(g) $\gamma_X = \gamma_Y = 0.01, \rho = 0.9, n = 4, \Phi_{XX} = \Phi_{YY} = 0.1$



(h) $\gamma_X = 0.01, \gamma_Y = 0.2, \rho = 0.9, n = 4, \Phi_{XX} = \Phi_{YY} = 0.1$



(i) $\gamma_X = \gamma_Y = 0.2, \rho = 0.9, n = 4, \Phi_{XX} = \Phi_{YY} = 0.1$

Figure 3. Empirical and approximated $F_Z^{-1}(p|\gamma_X, \gamma_Y, \omega, \rho).$

Alt Text: This figure contains nine blocks that show the curves of empirical and approximated $F_Z^{-1}(p|\gamma_X, \gamma_Y, \omega, \rho)$ whit respect to various combinations of $\gamma_X, \gamma_Y, \rho, \Phi_{XX}, \Phi_{YY},$ and $n.$

Table 9. In-control ARL values of the Shewhart-RZ control chart from Celano and Castagliola (2016a) designed with $ARL_0 = 200$ when the observations come from a VAR(1) model with $\Phi_{XX}, \Phi_{YY} \in \{0.1, 0.7\}, \Phi_{XY} \in \{0.01, 0.2\}, \rho_0 \in \{-0.9, -0.4, 0, 0.4, 0.9\}, \rho_1, n \in \{2, 5, 7, 10, 15\}$.

Φ_{XX}	Φ_{YY}	ρ_0	$(\gamma_X = 0.01, \gamma_Y = 0.01)$					$(\gamma_X = 0.2, \gamma_Y = 0.2)$						
			$n = 2$	$n = 5$	$n = 7$	$n = 10$	$n = 15$	$n = 2$	$n = 5$	$n = 7$	$n = 10$	$n = 15$		
0	0	-0.9	200	200	200	200	200	200	200	200	200	200	200	200
0.1	0.1	-0.9	141.62	107.65	99.57	98.34	93.27	133.7	109.40	103.65	97.06	95.13		
0.7	0.7	-0.9	31.67	8.93	7.31	5.76	5.13	32.43	9.18	6.91	5.97	5.15		
0	0	-0.4	200	200	200	200	200	200	200	200	200	200	200	200
0.1	0.1	-0.4	133.85	103.76	99.34	97.33	96.06	133.87	102.82	98.40	96.32	94.50		
0.7	0.7	-0.4	32.82	9.13	7.25	5.59	5.31	31.73	9.05	7.47	5.58	5.20		
0	0	0	200	200	200	200	200	200	200	200	200	200	200	200
0.1	0.1	0	140.10	102.28	99.21	86.90	95.87	140.03	103.20	95.24	94.71	97.13		
0.7	0.7	0	29.17	8.98	6.98	6.11	5.34	32.48	9.29	7.12	5.95	5.16		
0	0	0.4	200	200	200	200	200	200	200	200	200	200	200	200
0.1	0.1	0.4	135.90	106.62	99.48	95.65	91.74	135.89	104.09	96.36	91.28	90.06		
0.7	0.7	0.4	31.75	9.16	6.96	6.20	5.26	32.28	9.56	7.55	5.94	5.48		
0	0	0.9	200	200	200	200	200	200	200	200	200	200	200	200
0.1	0.1	0.9	140.01	106.03	101.60	98.63	95.82	137.23	106.05	101.65	96.38	95.23		
0.7	0.7	0.9	32.55	9.21	7.13	5.74	5.06	31.22	9.12	7.04	5.92	5.03		

Table 10. The front end (X_i) and back end (Y_i) pressures [psi] of the furnace for Phase I observations.

sample	X_i	Y_i	sample	X_i	Y_i	sample	X_i	Y_i	sample	X_i	Y_i
1	8.0	20.1	26	10.4	19.9	51	11.8	19.8	76	8.5	18.3
2	8.6	20.4	27	9.8	21.9	52	11.9	21.8	77	9.2	21.2
3	10.1	20.0	28	11.8	18.3	53	13.6	20.7	78	10.2	18.5
4	8.1	19.6	29	10.8	20.8	54	14.3	21.9	79	8.6	21.8
5	8.8	20.3	30	9.8	17.7	55	14.8	21.8	80	9.7	18.4
6	10.3	19.5	31	10.0	23.1	56	12.0	19.0	81	8.7	19.2
7	9.6	20.2	32	11.1	17.9	57	11.0	23.1	82	7.6	18.9
8	10.5	19.7	33	10.3	20.9	58	10.6	18.9	83	9.2	19.4
9	7.9	19.5	34	9.2	19.5	59	9.8	20.3	84	9.5	19.5
10	9.7	18.97	35	10.3	22.6	60	11.5	21.2	85	10.6	19.8
11	10.4	22.3	36	10.7	19.0	61	10.5	19.3	86	10.8	18.6
12	11.0	20.2	37	8.5	20.4	62	12.6	19.9	87	10.7	22.5
13	10.1	20.7	38	11.5	19.2	63	12.3	19.9	88	14.1	19.1
14	9.8	20.1	39	10.2	22.2	64	9.8	19.4	89	14.1	23.8
15	9.4	20.3	40	11.3	18.9	65	10.7	21.3	90	16.1	21.3
16	11.5	18.8	41	9.6	21.2	66	10.0	17.9	91	13.6	20.5
17	10.6	24.0	42	10.6	17.9	67	9.5	21.6	92	12.1	22.6
18	14.3	19.7	43	9.2	20.6	68	9.4	19.1	93	13.8	20.8
19	13.3	22.5	44	8.9	20.5	69	9.1	19.1	94	13.6	20.9
20	14.5	20.8	45	10.2	20.0	70	9.1	21.4	95	13.7	21.7
21	14.8	21.7	46	11.3	20.1	71	9.9	17.7	96	15.1	21.6
22	15.1	20.9	47	12.4	20.8	72	7.9	21.6	97	15.1	21.7
23	13.0	21.4	48	12.4	21.0	73	7.9	18.1	98	14.01	21.9
24	11.3	19.0	49	10.4	20.9	74	6.4	19.1	99	12.7	20.9
25	10.8	22.6	50	9.3	20.1	75	7.7	19.9	100	11.6	20.9

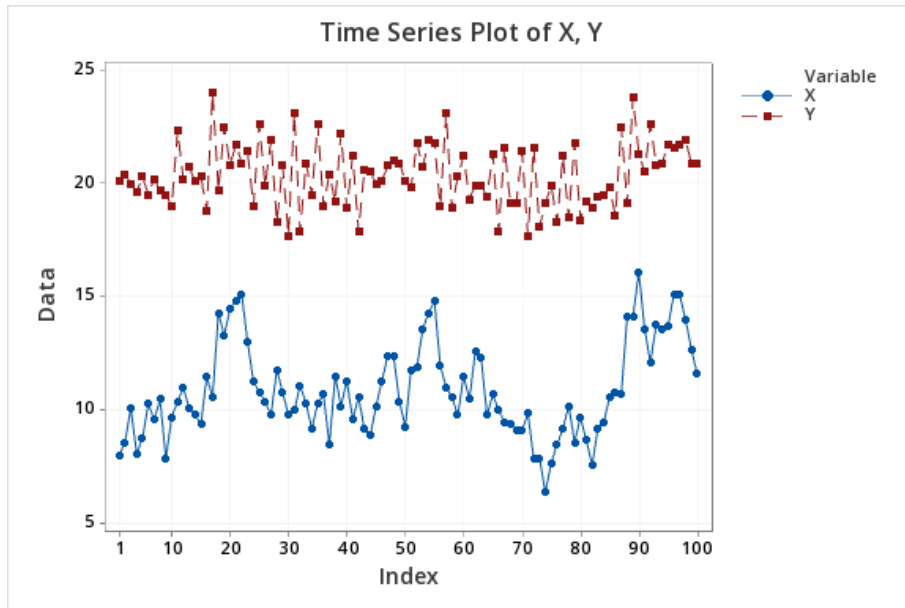
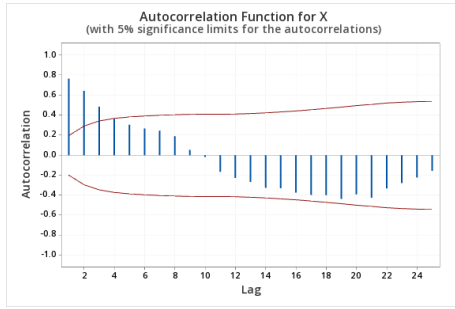
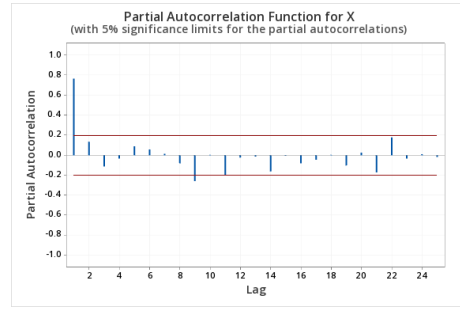


Figure 4. Time series plots of the pressure readings at both ends of the furnace (X: front end observations, Y: back end observations).

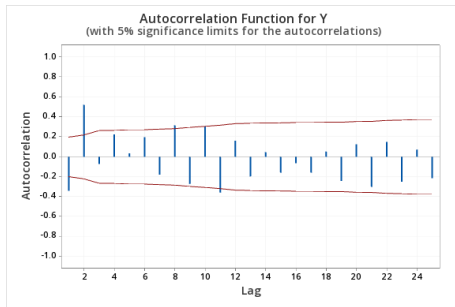
Alt Text: This figure shows the time series plots of the pressures at the front and back ends of the furnace in one figure.



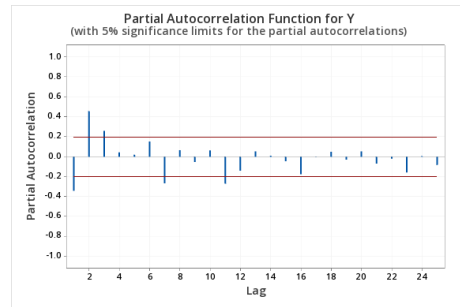
(a) ACF plot for X_t .



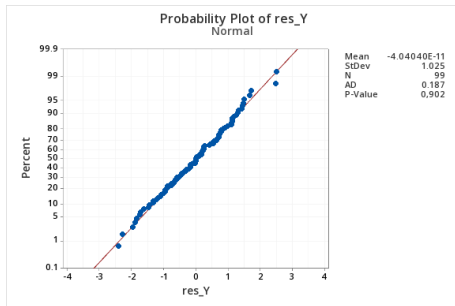
(b) PACF plot for X_t .



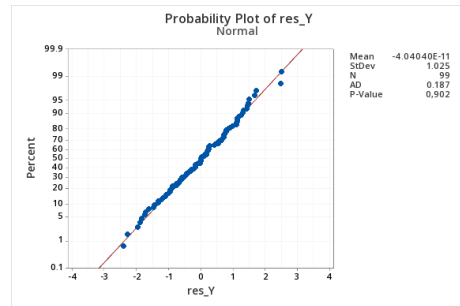
(c) ACF plot for Y_t .



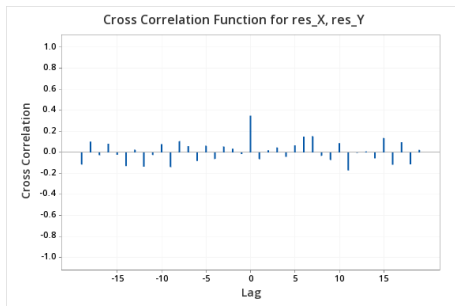
(d) PACF plot for Y_t .



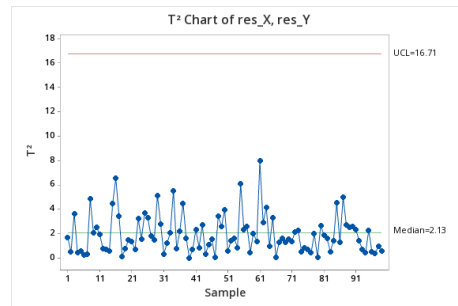
(e) Probability plot of X_t residuals.



(f) Probability plot of Y_t residuals.

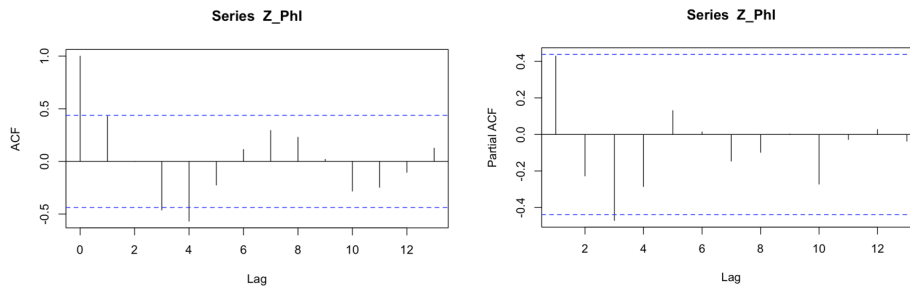


(g) Residual cross-correlation of VAR(1) model.



(h) Hotelling's T^2 chart for X_t and Y_t residuals.

Figure 5. Time series and stability study of the Phase I dataset of the industrial furnace example. Alt Text: This figure contains eight blocks and shows the results of the Time series analysis, including the ACF and PACF plots of individual time series along with the probability plots, the cross-correlation plot, and the Hotelling's T^2 chart for the residuals.

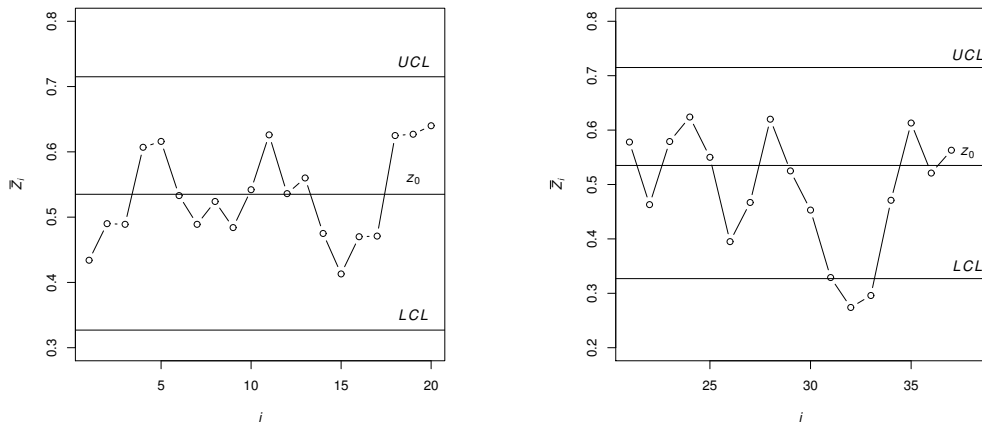


(a) ACF plot for \bar{Z}_i .

(b) PACF plot for \bar{Z}_i .

Figure 6. Sample ACF and PACF plots of \bar{Z}_i when $n = 5$.

Alt Text: This figure contains two blocks and shows the ACF and PACF plots of the monitoring statistics \bar{Z}_i when $n = 5$.



(a) Phase I control chart.

(b) Phase II control chart.

Figure 7. Shewhart-RZ control chart in Phase I and Phase II for the furnace example

Alt Text: This figure contains two blocks that display the Shewhart-RZ control charts in Phase I and Phase II for the furnace example.

Table 11. The front end (X_i) and back end (Y_i) pressures [psi] of the furnace for Phase II observations.

Sample	$X_{i,j}$ [psi]					\bar{X}_i [psi]	$\bar{Z}_i = \frac{\bar{X}_i}{\bar{Y}_i}$
	$Y_{i,j}$ [psi]					\bar{Y}_i [psi]	
21	12.2	13.0	11.9	10.9	11.8	11.96	0.578
	20.6	21.2	19.5	21.1	21.0	20.68	
22	9.5	9.3	9.3	8.6	8.9	9.12	0.463
	18.5	20.3	19.8	20.1	19.8	19.70	
23	10.3	11.4	11.8	13.1	12.7	11.86	0.579
	20.6	20.0	21.5	20.4	19.9	20.48	
24	13.9	12.4	12.5	14.3	13.5	13.23	0.624
	22.4	19.0	23.3	20.4	20.9	21.20	
25	13.0	11.7	12.0	9.6	7.4	10.74	0.550
	20.3	20.7	19.7	18.5	18.5	19.54	
26	7.0	8.2	7.5	7.0	9.10	7.76	0.395
	20.4	18.2	20.9	18.9	19.8	19.64	
27	8.6	8.9	9.8	9.6	10.3	9.44	0.467
	19.2	20.8	19.0	20.3	21.7	20.20	
28	11.9	12.4	12.2	12.9	14.3	12.74	0.620
	18.7	22.4	19.3	22.8	19.6	20.56	
29	12.9	12.1	10.1	10.2	7.6	10.58	0.525
	23.7	18.1	20.1	19.6	19.3	20.16	
30	7.8	9.0	10.8	9.4	7.8	8.96	0.453
	18.6	21.9	19.2	19.4	19.8	19.78	
31	8.0	5.8	5.5	6.5	5.2	6.20	0.329
	18.8	18.5	19.5	18.3	19.2	18.86	
32	5.0	4.3	4.5	5.5	5.7	5.00	0.274
	17.7	18.4	17.9	19.2	17.9	18.22	
33	3.8	5.9	6.7	6.8	5.2	5.68	0.296
	19.4	18.2	20.8	18.5	19.1	19.20	
34	6.3	9.1	9.3	10.4	11.9	9.40	0.471
	18.9	20.9	18.7	22.2	19.0	19.94	
35	12.4	14.6	13.6	13.1	10.1	12.76	0.613
	22.2	20.7	22.4	19.8	18.9	20.80	
36	10.1	11.0	11.4	11.0	10.0	10.70	0.521
	21.5	19.8	21.9	18.7	21.4	20.66	
37	11.3	10.6	11.7	10.7	13.6	11.58	0.563
	19.2	23.0	17.5	21.6	21.6	20.58	